Tutor/s

Dr. Carles Fité Piquer
Departament d'Enginyeria Química

Sr. Rodrigo Soto López
Departament d'Enginyeria Química

Màster en Enginyeria Química

Treball Final de Màster

Deactivation study of catalysts Amberlyst™ 35 and Purolite CT® 275 by acetonitrile

Estudi de la desactivació dels catalitzadors Amberlyst™ 35 i Purolite CT® 275 en presència d'acetonitril

Alberto Fernández Armisén
June 2015

Universitat de Barcelona

Dos campus d'excel·lència internacional
B:KC Barcelona Knowledge Campus
HUB^c Health Universitat de Barcelona Campus

Los científicos se esfuerzan por hacer posible lo imposible.

Los políticos, por hacer lo posible imposible.

Bertrand Russell

Me gustaría agradecer este trabajo a mi tutor Rodrigo Soto por su plena dedicación y su paciencia conmigo. Este trabajo no habría sido posible sin él y merece gran parte del mérito y mi infinito agradecimiento por todo lo aprendido a su lado.

También me gustaría agradecer a mi familia por proporcionarme las herramientas y el tiempo para poderlo llevar a cabo.

Por último agradecer al grupo de Cinética Aplicada y Catálisis por brindarme la oportunidad de trabajar con ellos y llevarme esta experiencia vital tan formativa y enriquecedora.

REPORT

CONTENTS

4. RESULTS AND DISCUSSION

8. ANNEXES

SUMMARY

Nowadays tertiary alkyl ethers are widely employed as high performance components for gasoline blending. This is because ethers enhance gasoline properties, such as octane rating. Ethers result essential to fulfil current environmental legislation, especially in more developed countries. For this reason etherification reactions have today an increasing interest for petrochemical industry.

The simultaneous liquid-phase production of ethyl *tert*-butyl ether (ETBE) and *tert*-amyl ethyl ether (TAEE) is the reaction system studied in the present work. These ethers are usually formed from ethanol (as common reactant) and isobutene (IB) for ETBE and isoamylenes (IA) for TAEE.

These olefins are part of the C_4 and C_5 cuts from Fluid Catalytic Cracking (FCC) or Stream Cracking units (SC). Usual impurities from these cuts are basic compounds such as acetonitrile (ACN) and amines. ACN is present in very low concentration but even at such low concentrations is the main cause of acid catalyst deactivation. Diffuse deactivation, means of acid sites neutralization, is one of the most important drawbacks that affect the catalyst lifespan of industrial reactors.

For the mentioned causes, it is therefore interesting to study the effect of the presence of ACN in the reactant streams on the catalysts used for etherification reactions. The catalysts used in this study are Amberlyst^{TM} 35 (A35) and Purolite CT® 275 (CT275), both widely employed in industrial etherification units.

1. INTRODUCTION

1. INTRODUCTION

1.1. IMPORTANCE OF FUELS

Since the birth of refining industry in the second half of XIX century, fuel has become the main energy source. The use of oil has been growing continuously and nowadays, the increase of the energy consumption has become a reality. This is synonym of an increasing depletion of oil reserves with the consequential problems.

Data of oil reserves, in thousands of millions of barrels, for the last years are shown in Table 1. The prediction about oil reserves in years (expressed as the ratio RR/P: being RR the reserves and P the annual production of oil derivatives) is also gathered in Table 1. This information is crucial to make estimations about the future.

Region	1988	1998	2007	2008	2008 [%]	RR/P [years]
North America	100	65.3	71.3	70.9	5.6	14.8
Rest of America	69.2	95.6	123.5	123.2	9.8	50.3
Europe and Eurasia	77.3	104.9	144.6	142.2	11.3	22.1
Middle East	653.0	684.3	755.0	754.1	59.9	78.6
Africa	59.0	77.2	125.3	125.6	10.0	33.4
Pacific Asia	39.9	41.3	41.3	42.0	3.3	14.5
TOTAL	**998.4**	**1068.5**	**1261.0**	**1258.0**	**100.0**	**42**
UE	8.3	8.9	6.7	6.3	0.5	7.7
OECD	118.3	89.2	90.3	88.9	7.1	13.2
OPEC	764.0	827.2	957.1	955.8	76.0	71.1
Non-OPEC	173.5	157.6	174.7	174.4	13.9	14.8
Old URSS	60.9	83.8	129.2	127.8	10.2	27.2

Table 1. Oil crude reserves in thousands of millions of barrels [1].

Oil is essential for transportation among other things. About 57% of this oil was consumed for transportation purposes in 2007 [2]. The analysis of these data indicate a energy crisis in the forthcoming years because oil reserves are extinguished.

The Organization of the Petroleum Exporting Countries (OPEC) is the most important organization of petroleum exporters. It was founded in Bagdad in 1960 and the founding members were Iraq, Iran, Venezuela, Saudi Arabia and Kuwait. These countries were later joined by Qatar (1961), Indonesia (1962), Libya (1962), the United Arab Emirates (1967), Algeria (1969), Nigeria (1971), Ecuador (1973), Gabon (1975) and Angola (2007) to constitute a total organization of twelve members [3]. As seen in Table 1, these countries control the 76 % of the total petroleum reserves.

1.2. EMISSIONS AND GASOLINE REFORMULATION

In the United States, the Clean Air Act Amendments (CAAA) of 1990 increased the severity of legislation concerning emissions limits of vehicles and required the manufacture of cleaner fuels, including reformulation of gasoline [4]. This fact started a new mentality that was moved to Europe, where governments make more rigorous legislation and restrictions regarding control of emissions and environmental concerns. In order to reduce undesirable emissions and to accomplish the more and more restrictive legislation, both in fuel composition and exhaust emissions, some solutions have been introduced. The most important change in fuel reformulation was the banning of lead from antiknocking compounds used in gasoline due to its high toxicity. To accomplish normative maintaining the octane number, some substitutes were proposed with appropriate properties: total solubility in fuel blends –so they would be hydrocarbons- and heteroatom presence in their structure –nitrogen, oxygen or metals-. The organometallic compounds were rejected because of their toxicity, cost and instability. Besides, nitrogen derivatives partial oxidation results in a nitrogen oxides (NO_X) production increase. Thus, oxygenates were chosen as new fuel additives.

Last EU Directive 2009/30/CE has increased oxygenates maximum level up to 3.7%wt in oxygen content, increasing maximum introduction of both ethers and alcohols except methanol respect previous Directives. This measure seems to be the definitive promotion of direct and/or indirect addition of oxygenates compounds in gasoline, especially those obtained from biomass sources [5].

The limit composition of some compounds used for reformulated gasoline (since 01-02-2011 by EU Directive 2009/30/CE) is shown in Table 2.

Parameter	Max or min value	Units
RON	95 (min.)	
Rvp	60 (max.)	KPa
Olefins	18 (max.)	vol.%
Aromatics	35 (max.)	vol.%
Benzene	1 (max.)	vol.%
Oxygen	3.7 (max.)	wt.%
Alcohols	55 (max.)	vol.%
Ethers	22 (max.)	vol.%
Another oxygenates	15 (max.)	vol.%
Lead	0.005 (max.)	g/L
Sulfur	10 (max.)	Ppm

Table 2. New formulation of gasoline blending by EU Directive 2009/30/CE [5].

The composition of gasoline is different depending on the country and also depending on the weather and the season, but countries belong Europe Union (EU) have to fulfil these limit values.

Table 3 shows the evolution of gasoline fuelled car emissions.

Date	CO	VOC	NO_X
July 1992	2.72	-	-
January 1996	2.2	-	-
January 2000	2.3	0.2	0.15
January 2005	1.0	0.1	0.08
September 2014	1.0	0.1	0.06

Table 3. Evolution of gasoline passenger car emissions in [g/Km] [5].

The most important contributions of oxygenates are a better combustion yield by the oxygen presence that results in a reduction of emitted volatile organic compound (VOC) and carbon monoxide (CO). Furthermore, adding oxygenates improves octane number because oxygenates are anti-knocking substances. However, more complete combustion by increasing the oxygen content could result in increasing emissions of NO_X. Among the different oxygenates – alcohols, carboxylic acids, ketones, ethers, esters or phenols-, only alcohols and ethers are used in gasoline and esters in diesel due to their low cost, easy handling and transportation, and high chemical resemblance with other blending compounds.

1.3. OXYGENATES FUELS

Oxygenates fuels are hydrocarbons containing oxygen within the chain of carbon and hydrogen atoms. There are two main types of oxygenates used for gasoline blending: alcohols as methanol (MEOH), ethanol (EtOH), *tert*-butyl alcohol (TBA), *tert*-amyl alcohol (TAA) and tertiary alkyl ethers. Among ethers, the most widely used are ethyl *tert*-butyl ether (ETBE), methyl *tert*-butyl ether (MTBE), *tert*-amyl ethyl ether

(TAEE), and *tert*-amyl methyl ether (TAME). The properties of main oxygenates fuels employed in reformulated gasoline blending are shown in Table 4.

Properties	**MTBE**	**ETBE**	**TAME**	**TAEE**	**EtOH**
(RON*+MON**)/2	110	112	105	100	115
Rvp pure [psi]	7.8	4	2.5	-	2.3
Rvp in blend [psi]	8	4	2	1.5	18
Boilling point [ºC]	55	72	86.3	111.1	78.3
Oxygen content [% weight]	18.2	15.7	15.7	13.8	34.8
Energy content [MTBU/Gal]	93.5	96.9	100.6	-	76
Oxygenate solubility in water [%wt]	4.3	1.2	1.15	0.49	Infinite
Water solubility in oxygenate [%wt]	1.4	0.5	0.6	0.28	Infinite

Table 4. Properties of main oxygenates fuels (*RON = Research Octane Number/**MON = Motor Octane Number) [5].

Ethers are preferred to lighter alcohols by refiners for several reasons: because of their low blending Reid vapor pressure (Rvp) which means a reduction in the evaporation of VOC's; low vaporization latent heats; low oxygen contents, which improves oxygen dispersion, and because they avoid phase separation in the presence of water, which accounts for their full compatibility in the petroleum refining and distribution systems [6]. Ethanol addition, however, present some advantages like gasoline additive: it could be obtained from land crops with no fossil petrol origin at all, and presents a rapid and complete biodegradability and a well-known toxicity in fauna and flora [5].

The main drawback of using ethers can be the production of aldehyde emissions because such compounds present a very high atmospheric reactivity. The presence of ternary alcohols like TBA or TAA (obtained by the addition of water to isobutene or isoamylene respectively) in the blending contributes to reduce this problem. Both alcohols have a very low atmospheric reactivity and also low aldehyde emission which can be explained if consider that the carbon linked to the oxygen atom doesn't contain any hydrogen which is required to directly produce aldehydes during combustion. It is important to notice that aldehyde emissions from ethers are lower in the presence of these alcohols. On the other hand, the water solubility of both alcohols is much lower than that of the lighter alcohols; even TAA in the pure form shows some insolvency with water. Furthermore a gasoline blended with a mixture of ethers and these alcohols should be shippable on pipelines. In comparison to lighter alcohols, TBA and TAA have low blending Rvp because the azeotropes that they form with gasoline hydrocarbons are in the mid to higher boiling range of the gasoline distillation curve. As a result, this effect helps to improve the “cold driveability” by making easier the vaporization and combustion of the higher boiling hydrocarbons of gasoline [7].

In many countries ethers are widely used, especially in Europe, based on the good properties they present.

1.4. ETHERS: MTBE, ETBE, TAME and TAEE

There are several ways for obtaining ethers such as dehydration of alcohols. Some examples of this chemical pathway are the formation of ETBE from TBA and ethanol, the formation of TAEE from TAA and ethanol and the formation of diethyl ether (DEE) from ethanol over sulphonic ion exchange acid catalysts [8].

Another chemical pathway (more employed in chemical plants) to produce tertiary alkyl ethers is by the addition of primary alcohols to tertiary olefins over acid catalysts. An example of this synthesis route is MTBE synthesized from methanol and isobutene (IB) as is illustrated in R1 [6].

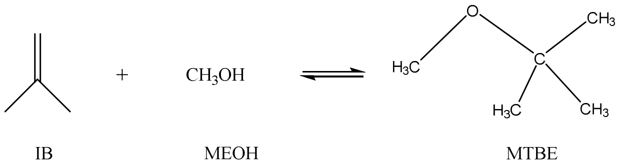

R1

MTBE is the first main oxygenated fuel used for gasoline blending for many reasons as the affordable reactants and the low cost of methanol derived from natural gas (NG). However, in the last decades ETBE market have been growing (is shown in Figure 1) because of the groundwater contamination caused by MTBE. Furthermore, it has been shown that commercial MTBE plants can easily be revamped into ETBE, only by introducing slight modifications. Some refiners are interested in shifting MTBE to ETBE production or vice versa, depending on the market prize of alcohols. The world’s largest MTBE plants have been converted for full ETBE flexibility [6]. ETBE is obtained from ethanol addition to IB, as is illustrated in R2 [9, 10].

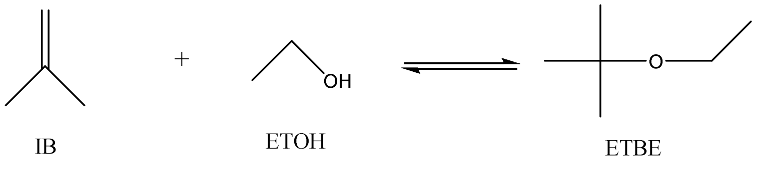

R2

Ethanol can be obtained from oil or from biomass fermentation, thus called bioethanol. It is to be highlighted that ETBE produced from bioethanol is considered a biofuel. EU Directive 2009/28/CE promote the use of renewable energies like biofuels

[9]. This means that ETBE would help to reduce the dependence on methanol and oil importations.

In other hand, TAME and TAEE not employ IB as olefin source. These ethers are formed by addition of alcohol to isoamylenes (IA). These olefins present two reactive isomers: 2-methyl-2-butene (2M2B) and 2-methyl-1-butene (2M1B). The isomerisation equilibrium reaction (R3, [9]) favours 2M2B formation (is more stable and less reactive [9]), but as reaction advances and 2M1B is consumed, the reverse reaction is favoured.

Isoamylenes present some disadvantages as a component of gasoline, particularly in tropical zones. This is because these are the olefins with the highest Rvp, the highest atmospheric reactivity, the highest potential of tropospheric ozone formation (around 90%) and these are the largest amount of the olefins present in a gasoline: above 25 wt% of the C_5 fraction from Fluid Catalytic Cracking (FCC) [9]. To diminish the impact of their use as fuel components on the environment, the reduction of the IA content by means of either its etherification with primary alcohols obtaining TAME and/or TAEE or via oligomerization or alkylation would result in a more suitable alternative than the reduction of the total olefin content of a gasoline [9].

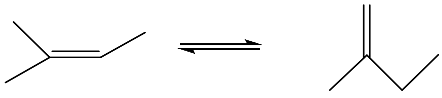

2M2B 2M1B

R3

TAME is obtained from methanol (as MTBE) and IA as is shown in R4. TAME is not seen as a rival of MTBE despite the fact that it uses the same alcohol as raw material, since TAME is made by combining methanol with isoamylenes of C_5 cut, more expensive reactive than isobutene [7], but TAME presents much lower Rvp than MTBE (as is shown in Table 4) and it results interesting in some warm countries, especially in summer time.

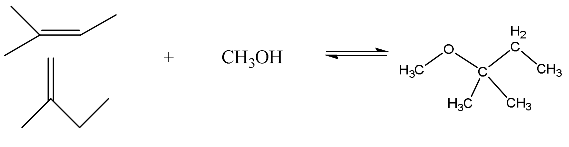

IA MEOH TAME

R4

TAEE is produced from isoamylenes and ethanol as is illustrated in R5 [9]. Then, TAEE obtained from bioethanol is considered a biofuel too.

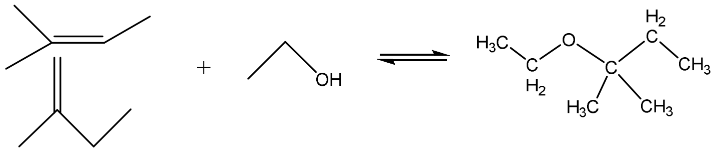

IA ETOH TAEE

R5

In Europe, the current demand for fuel ethers is about six millon of tones per year. Despite the increasing amount of ethanol direct blending, the ETBE market still shows a positive trend, as shown in Figure 1. TAEE started to be produced in important amount recent years, as also shown Figure 1.

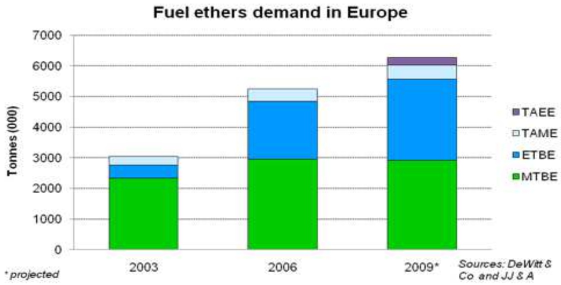

Figure 1. Fuel ethers demand in Europe [11].

Ethers production in Europe is widely distributed around the continent. The main production units in Europe and Spain are shown in Table 5.

Country	Localization	Ether	1000 Tm/year
Germany	Marl	MTBE	250
Germany	Karlsruhe	ETBE	163
Germany	Schwedt	TAME	160
Holland	Botlek	MTBE	591
Holland	Geleen	ETBE	138
Holland	Pernis	MTBE	153
Italy	Sarroch	TAME	237
Italy	Ravena	ETBE	133
Belgium	Antwerp a	ETBE	183
Belgium	Antwerp b	MTBE	270
France	Fos sur Mer	ETBE	612
Spain	Algeciras	ETBE	54
Spain	Bilbao	ETBE	74
Spain	Huelva	ETBE	50
Spain	A Coruña	ETBE	52
Spain	Puertollano	ETBE	67
Spain	Tarragona a	ETBE	54
Spain	Tarragona b	ETBE	71

Table 5. Main units production of ethers in Europe and Spain in 2005 [11].

There are other interesting ethers due to their properties but less common as isopropyl *tert*-butyl ether (IPTBE) and diisopropyl ether (DIPE) [1].

1.5. ETBE and TAEE LIQUID-PHASE SYNTHESIS

As mentioned before, the main industrial chemical pathway for producing ETBE and TAEE consists in the addition of ethanol to tertiary olefins, isobutene and isoamylenes (R1 and R5). The reactions are reversible and exothermic (ΔH^o_R (298.16 K) = -36.3±1.3 [KJ/mol] for ETBE [9], ΔH^o_R (298.16 K) = -35.1 ±6.0 [KJ/mol] for TAEE from 2M1B [9] and ΔH^o_R (298.16 K) = -25.5 ±3.0 for TAEE from 2M2B [9]; in all cases $\Delta H^o_R < 0$ confirming that such reactions are exothermic). These reactions are usually catalysed by macroporous sulfonic acid resins within a working temperature range from 40 to 80 ºC. Under these operating conditions the selectivity is very high, but some by-products could be formed if working temperature is high or if initial molar ratio between alcohol and olefin is not near at stoichiometric. These byproducts are produced by side reactions.

ETBE and TAEE production rates are strongly lowered by the initial water presence. Water acts with inhibitor effect and as a competitor with alcohol for the olefins reactions as shown in R6 and R7 [12]. No presence of water in raw materials (only ethanol, olefins doesn't contain water) is the ideal situation, but this is not real. The residual water content at equilibrium (by the azeotrope with ethanol) is rather small but never null, and is impossible to remove all water content.

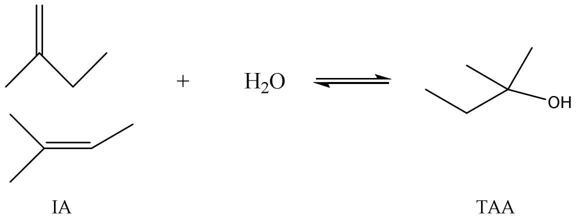

R6

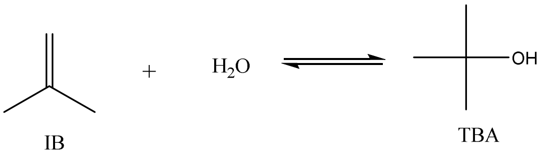

R7

There are many byproducts produced by oligomerization as are illustrated in R8, R9, R10 and R11 [11, 12]. For example $C_{4\text{-}5}$ codimers include 2,4,4-trimethyl-1-hexene, 2,4,4-trimethyl-2-hexene, 2,3,3-trimethyl-1-hexene, etc. Excess of olefins and high temperatures enhances oligomerization reaction rates. For these reasons in industrial process slight excess of ethanol is usually used to avoid it and to increase olefins conversion. Water presence also acts as inhibitor in the oligomerization reactions as a result of the competition for the catalytic active sites [12].

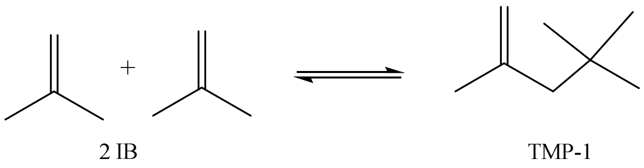

R8

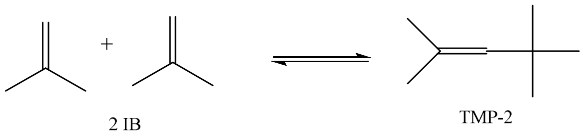

R9

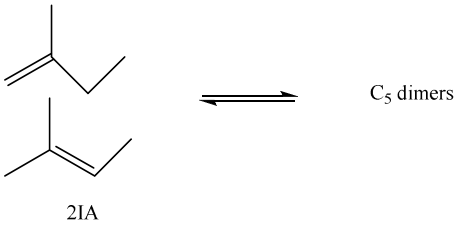

R10

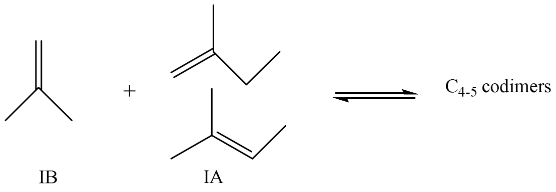

R11

Dehydration of ethanol is another example of side reaction shows in R12 [13].

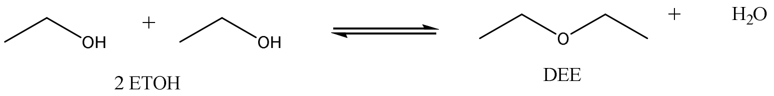

R12

The simultaneous etherification of isobutene and isoamylenes could constitute the integration of two etherification processes at industrial scale, which would mean savings in installation, maintenance and operating costs. The etherification of gasolines from FCC has already been studied showing as feasible the technique of the simultaneous etherification of several olefins [9].

1.6. KINETIC OF CATALYSED ETHERIFICATION REACTIONS

The most interesting characteristics of etherification with solid catalyst are explained in this section.

Kinetics of liquid-phase synthesis of ETBE (R2) was studied previously. The main conclusions of these previous studies [14] are:

1) Isobutene has an enhancing effect on the reaction rate.
2) Ethanol has an inhibitor effect on the reaction rate.

3) Low ETBE concentrations enhance reaction but approaches reaction to equilibrium. Then, ETBE can be considered as an inhibitor.

1.6.1. Mass resistances

Etherification catalyzed implies different steps for reactants: diffusion from bulk phase to external catalyst surface through external film; diffusion inside the catalyst porous; adsorption on active sites and reaction over active center. For products the way is the opposite: desorption of active sites; diffusion from porous to external catalyst surface and diffusion from external catalyst surface to bulk phase. Diffusion in external film is named external mass transfer (EMT). Diffusion through the catalyst pores is named internal mass transfer (IMT). To study intrinsic reaction rate, EMT and IMT should be avoided. This means both steps have to be fast enough to ensure control by surface reaction. To achieve it the next sentences must be followed:

1) To avoid IMT is important to control particles diameter since particles with a big diameter could show effect of IMT. A correct range of particle diameter (Dp) must be selected. Figure 2 shows profile of temperature and concentrations of reactants and products for exothermic reactions.

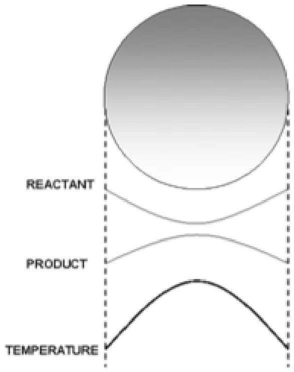

Figure 2. Concentration and temperature profiles in a spherical solid [5].

2) To avoid EMT is important to control the flow. There are two possible cases, depending on the type of reactor. If the reactor is a stirred tank reactor, the stirring speed must be fixed in a big value. If the reactor is a tubular reactor, the liquid hourly space velocity (LHSV) must be fixed also in a big value. Figure 3 shows concentration and temperature profiles along the external film.

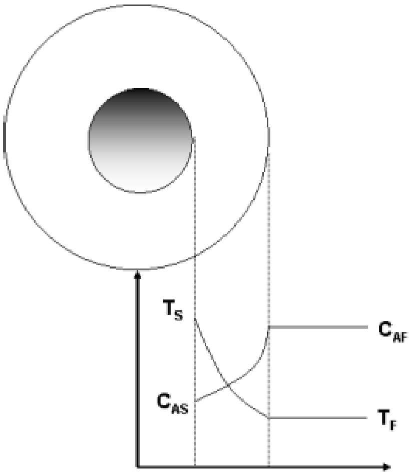

Figure 3. Concentration and temperature profiles along the external film [5].

Concentration of reactant at surface (C_{AS}) tends to zero when EMT is the limiting step. In opposite case, C_{AS} tends to concentration of reactant inside fluid phase (C_{AF}).

Figure 4 illustrates the dependence between reaction rate and Dp (when only IMT are considered) or LHSV (only when EMT effects are considered).

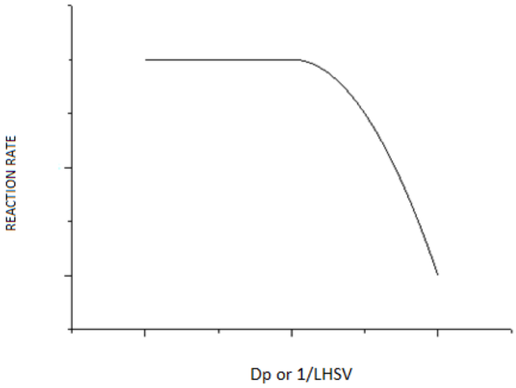

Figure 4. Trend of reaction rate for different values of Dp and LHSV.

The first constant period indicates the control of the reaction rate. Reaction rate is constant and it does not depend neither on the Dp nor on the LHSV.

There is a maximum value for Dp to avoid IMT: for larger particles, reaction rate depends on particle's diameter.

There is a minimum value for LHSV to avoid EMT: for lower values of LHSV reaction rate depends of LHSV.

LHSV is calculated as volumetric flow (Q) divided for volume of reactor bed (V_B). LHSV presents units of [time^{-1}]. A similar parameter is weight hourly space velocity (WHSV). WHSV is calculated as mass flow (W) divided by catalyst mass (M_C).

Equations for calculate these two parameters are present below.

$$\mathrm{LHSV} = \frac{\mathrm{Q}}{\mathrm{V_B}}$$

Equation 1

$$\mathrm{WHSV} = \frac{\mathrm{W}}{\mathrm{M_C}}$$

Equation 2

1.6.2. Design Equation in Fixed Bed

Equation 3 illustrates the design equation in a catalytic fixed bed [15] without products in feed stream. Equation 3 relates reaction rate of component *j* (r_j), conversion of reactant *j* (X_j), molar inlet flow of component *j* (F_j^{inlet}) and M_C.

$$\frac{M_C}{F_j^{inlet}} = \int_0^{X_j} \frac{dX_j}{-r_j}$$

Equation 3

1.6.3. Kinetic Regimes

There are two types of kinetics regimes in etherification catalysed reactions that present different performance.

1) *Differential regime*. It is widely accepted that differential regime for these etherification reactions occurs when reaction conversions are lower than 10% [5]. There are several ways to accomplish this conversion: use of low activity catalyst; use inert fluids in feed stream or employ mixture of catalyst and inert [16]. A differential bed usually consists of a fixed bed composed by a homogeneous mixture of small amount of catalyst diluted with particles of inert component of the same size. The presence of inert is important to avoid bed fluidization and to enhance heat transmission, ensuring isothermal profile in reactor, but it presents some disadvantages: distribution of activity if mixture isn’t homogeneous; change the residence time or appearance of bypass inside reactor [16]. Differential regime presents an advantage due to the low extent of the reaction that takes place along the reactor, it can be considered isothermal, as the small amounts of heat generated by the reaction can be easily removed by the system. Isothermal system is needed to obtain intrinsic reaction rate at known temperature. Equation 3 can be simplified under differential conditions: reaction rate can be considered constant. Equation 4 [15] shows this simplification.

$$\frac{M_C}{F_j} = \int_0^{X_j} \left(\frac{dX_j}{-r_j}\right) = \frac{X_j - 0}{-r_j} \qquad \text{Equation 4}$$

Reordering Equation 4, Equation 5 is obtained.

$$X_j = r_j \cdot \frac{M_C}{F_j} \qquad \text{Equation 5}$$

2) *Integral regime*. Integral regime is employed in industrial units. Implies high conversion and reactor catalytic bed completely loaded with pure catalyst (without inert). Temperatures profile is manifested because reaction heat cannot be completely removed. Then, temperature inside the reactor rises and the selectivity decreases, implying non-desirable byproducts formation. Furthermore, high temperatures enhance the reaction, rate but decrease equilibrium conversion (X_{eq}).

Figure 5 plots a typical graph where Xj as y-axis and coefficient ($\frac{M_C}{F_j}$) as x-axis, r_j is the slope of the curve.

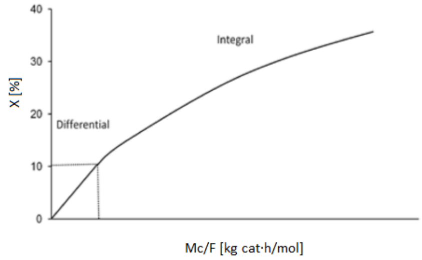

Figure 5. Trend of conversion versus ($\frac{M_C}{F}$) [5].

At low conversion, that is, under differential regime, the slope of the curve can be considered as constant (curve approaches a straight line), so r can be easily estimated (Equation 5). The range of conversions up to 10% belongs to differential regime, conversions higher than 10% belong to integral regime.

1.6.4. Kinetic Models

There are two classical kinetics models for reactions catalyzed by solids: Langmuir-Hinshelwood-Hougen-Watson (LHHW) and Eley-Rideal (ER) models.

Surface reaction is usually considered as the rate limiting step in reaction models over porous solids. The developed kinetic expressions for these models are based on the following assumptions [5]:

1) The solid surface contains a fixed number of active sites.
2) All the active sites are identical.

3) The active sites reactivity does not depend on quantity and nature of the rest of compounds present on the solid surface during the reaction, it only depends on temperature.

LHHW equations come from Langmuir isotherm development using species concentration near from active sites instead of occupied sites fraction (Langmuir and Hinshelwood) or surface molar concentrations (Hougen and Watson), which are difficult to determine experimentally. In LHHW formalism, adsorbed reactants react to give adsorbed product, which later desorbs from the active site. However, ER (Eley-Rideal) mechanisms do not consider the adsorption of all the reactants, so in this case reaction occurs directly between an adsorbed reactant molecule with reactant molecules present in fluid phase. In both cases, in absence of external and internal mass transfers, general procedure consists of proposing a determining step (reactants adsorption, products desorption or surface reaction), and then to develop equations depending on possible different active sites involved in the catalytic process. It normally exist many different possible kinetic models to explain reaction data, but all of them present the same general structure illustrate in Equation 6 [5].

$$r=[\text{kinetic term}]\cdot[\text{Catalyst actvivity term}]\cdot\frac{[\text{Potential term}]}{[\text{Adsorption term}]} \qquad \text{Equation 6}$$

Both models are represented by the reaction mechanisms illustrated in Figures 6 and 7. Reactants are represented by A and B; product is represented by P and active centre is represented by θ (when θ appears with a letter means adsorbed reactant or product).

$$A+\theta\rightarrow A\theta$$
$$B+\theta\rightarrow B\theta$$
$$A\theta+B\theta\rightarrow P\theta+\theta$$
$$P\theta\rightarrow P+\theta$$

Figure 6. LHHW mechanism [15].

$$A+\theta\rightarrow A\theta$$
$$B+A\theta\rightarrow P\theta$$
$$P\theta\rightarrow P+\theta$$

Figure 7. RE mechanism [15].

Based on previous kinetic studies, the best kinetic model for ETBE stems from an ER mechanism [14] but for TAEE the best kinetic model stems from LHHW mechanism [17].

1.7. ETHERIFICATION CATALYST

Etherification reactions need protons presence to occur which are provided by the acid catalyst. This type of catalysis is heterogeneous because reactants (usually in liquid-phase) are in different phase than catalyst (resin, solid phase). Heterogeneous catalysts offer several advantages over homogeneous, both from technical and environmental standpoints: low equipment corrosion, easy product separation, low potential pollution in waste streams and recycling of catalyst. Moreover, using a solid catalyst it is possible to carry out liquid or vapor phase synthesis on a fixed or fluidized bed process. Then, heterogeneous catalysis is indeed shown as the best option for industrial procedures. There are several types of acid solid catalyst that can be used for etherification, but in the range of operating temperature ion-exchange resins offer the best performance. [5].

Ion exchange resins consist of organic solids formed by a polymeric matrix and an ensemble of functional groups which are bonded to the matrix. The polymeric matrix is an irregular three-dimensional hydrocarbon chains structure with hydrophobic character, while functional groups are of hydrophilic nature [5]. Ion-exchangers resins can be divided by functional groups into cation-exchange resins (polyacids), anion-exchange resins (polybases), and amphoteric or bipolar resins (polyampholites). The firsts may be either of strong acid or weak acid type; the seconds may be either strong base or weak base type. If the electric charge carriers in the molecular network of an ion-exchange resin are fixed ions (ionogenic or functional groups) of a single type, such as sulphonic acid groups, the ion-exchange resin is called monofunctional. However, if the resin contains ionogenic groups of various types, it is called polyfunctional [18].

Ion exchange resins are insoluble in organic solvents due to its structure, unless those can break C-C bonds. According to their chemical structure, resins have different chemical, thermal and mechanical stability, being the key parameters their cross-linking degree and the functional groups nature. The space limited by the polymeric chains is called resin pore volume, and it can vary depending on the medium-resin interaction. When resins are in contact with chemical mixtures, they can adsorb them and swell. That phenomenon depends on both the resin nature and medium polarity. If the reaction medium contains different species, the more solvating ones will be preferably adsorbed.

The solid catalysts that are commonly used in ether synthesis are polisulfonated styrene-divinylbenzene (DVB) resins. They are classified in two groups depending on the synthesis process, which provides them very different properties:

1) Microporous or gel-type resins are homogeneous. Ion exchange in a gel-like resin-solution system is possible as a result of diffusion of ions undergoing exchange through the molecular network of the swelled ion exchanger.

   This type of resins are obtained by suspension polymerization at high temperatures catalyzed by organic peroxides and using DVB as cross-linker, which creates a 3D insoluble structure placing itself among styrene chains (Figure 8) and provides stiffness and mechanical resistance. This process leads to a microporous structure. These resins are generally low cross-linked (1-8% DVB [5]) and present a low surface area at dry state, but their porosity can increase substantially due to swelling in polar solvents. Their pores, called micropores, are very small (0.2-0.7 nm [5]), and only appear in the swollen state.

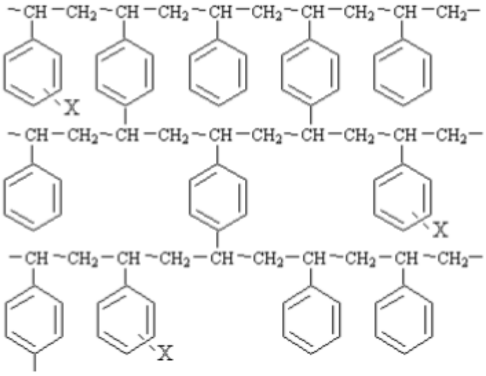

Figure 8. DVB functionalized matrix where X=functional group [5]

2) Macroporous resins are heterogeneous. They are normally depicted as an ensemble of microporous particles interspersed by permanent pores. They have large DVB amounts (5-30%). In order to obtain the macroporous structure, the presence of diluents -also called porogens- during the polymerization, such as heptane or toluene [5], is necessary. Such porogens are included selectively inside the polymer matrix and avoid local growing by phase separation effect. As a result, when diluents are extracted, permanent porosity remains in the resin. Therefore, three different types of pore families are observed in macroreticular resins:

   1. Micropores: inside the microspheres (10-30 nm) there is the first family of smallest pores (< 5 nm), which are responsible for the high surface

area of this materials; these microspheres form microgel clumps (gel-spheres agglomerates).

2. Mesopores: between the microspheres exists another family of intermediate diameter pores (8-20 nm), which may account for moderate surface areas.
3. Macropores: a third family of large pores with diameter 30-80 nm is located among the agglomerates, which yield very low surface area but large pore volume (up to 3 mL/g [5]).

Macropores are permanent and can be detected by standard techniques of pore analysis, e.g. adsorption-desorption of nitrogen (N_2) at 77 K, while meso and microporous, which appear only in swollen state, are non-permanent and can be detected by characterization techniques in liquid media, such as Inverse Steric Exclusion Chromatography (ISEC) [5].

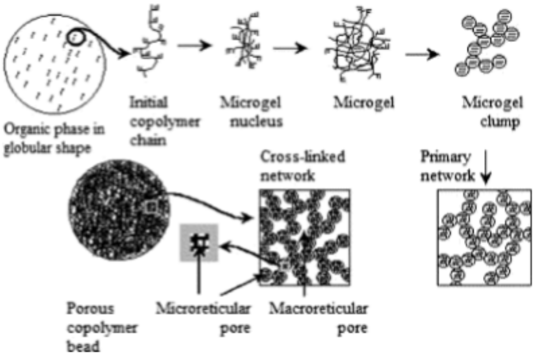

Figure 9. Mechanism of porous structure formation during suspension copolymerization of styrene-DVB [5].

1.8. CATALYST LIFESPAN AND DEACTIVATION

Catalyst's life span is one of the most important aspects to consider in industrial reactors. There are several reasons for catalyst's deactivation. Activity decay of the catalyst can be originated by the adsorption of metal ions, by the blockage of the functional groups by polymeric products, by the formation of stabilized chemical compounds or by thermal loss of functional groups due to hot spots in the reactor.

All these types of catalyst deactivation are explained [5]:

1) *Ion exchange*: This phenomenon occurs when ions are present in the reactor feed. Cations deactivate etherification catalysts by exchange with the catalytic proton, as is illustrated in Figure 10.

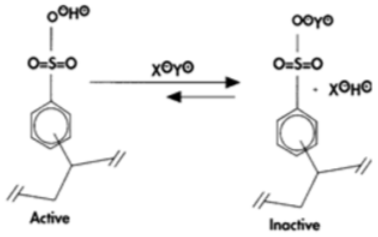

Figure 10. Salt deactivation of etherification catalysts [5].

2) *Desulfonation*: This type of deactivation occurs by temperature effect. The C-S bond between functional groups and matrix can be broken by thermal stress. Thermal stress causes thermal processes such as pyrolisis, hydrolisis, sulfone bridging formation and sulfonic ester formation. These processes are considered and planned in industrial unit: temperatures over 76 ºC cause desulfonation rates of 10% annually and for temperatures over 100ºC the ratio of desultonation rates increases about 1.8 fold for each increase of 10ºC [5]. Desulfonation mechanism is illustrated in Figure 11.

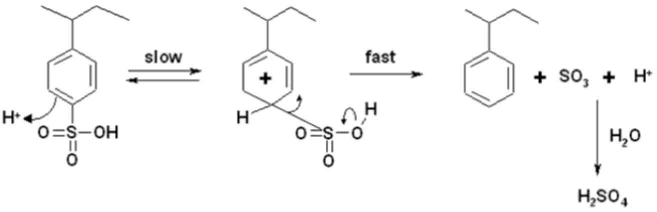

Figure 11. Thermal decomposition of strongly acid resin catalyst [5].

3) *Deposition*: Phenomenon of deactivation via surface fouling is caused by heavy oils, waxes, greases and polymers [5] as shown in Figure 12. These components arise of the polymerization of dienes, isobutylenes and linear butenes current in feeds from FCC. This type of deactivation leads to a permanent loss of capacity and the reduction of pore volume and diameter. Cleaning of the resin by washing with organic solvents is usually not efficient and the catalyst must be replaced.

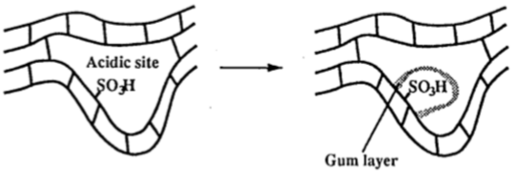

Figure 12. Gun formation around active site [5].

4) *Decrosslinking of resin matrix*: The matrix is decrosslinking by exposition to oxidizing agents such as chlorine, Fe^{3+}, Fe^{2+}, O_2, etc. This exposition also causes

swelling of the resin beads. Then, diffusion of reactants inside the matrix is affected (Figure 13). Damage is irreversible and catalyst needs to be replaced.

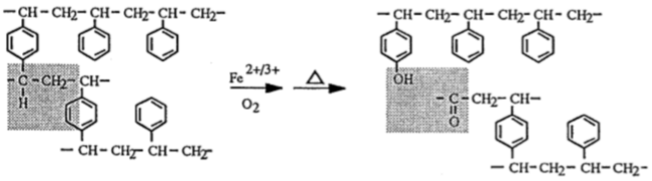

Figure 13. Decrosslinking of a resin matrix with rust, oxygen and heat [5].

5) *Neutralization*: Neutralization of sulfonic groups is an important cause of deactivation. This is commercially evidenced by the fact that in fixed bed reactor systems, a catalyst which is 40% neutralized can be considered commercially dead. It has been reported that neutralization of about 10% of the sulfonic groups originated an activity decrease of about 30% [19]. Lewis bases (electron donating species) deactivate the catalyst by reacting with the catalyst's sulfonic acid proton to form inactive conjugate salts such as ammonium and sulfonium products. Neutralization mechanism with ammonia, forming ammonium component, is shown in Figure 14. The activity lost by neutralization can be recovered by clorhidric acid regeneration.

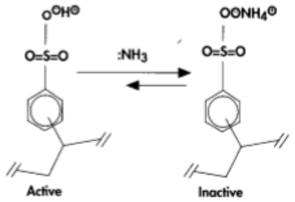

Figure 14. Neutralization of catalyst sulfonic acid proton [5].

This type of deactivation occurs by bases presence. These bases generally arise from nitrogenous or sulfurous compounds which are commonly latent in FCC and crude C_4 streams [5]. There are two great types of bases in feedstock: strong bases and weak bases, which generate two types of deactivation.

The first type, named plug flow deactivation, is generated by strong bases [20]. These neutralize directly the active centre of the resins and leads to a plug flow profile of the catalytic activity decay along the catalytic bed. Deactivation start in reactor inlet, and continue along the reactor, what means that if catalytic bed is long enough, when deactivation start, there is no evidence in the reactor outlet because conversion outside is the same until conversion falls suddenly. At this moment, the reactor volume deactivated is sufficient to affect conversion outside the reactor. An example of this case of deactivation is produced by monomethylamyne (MMA) [20].

The second, named diffused neutralization or smooth deactivation, not neutralize directly the active centre of the resins. Weak bases react with water (hydrolysis) or alcohol (alcoholysis) to form another basic compound. These formed compounds are stronger bases than the original and neutralize sharply the sulphonic groups. This type of neutralization is uniform along the reactor bed as they are also absorbed uniformly along whole the bed reactor. It means that activity drop is continuous along the time since deactivation started. Acetonitrile (ACN) belongs to this second type of deactivators [20]. ACN is a residual compound from butadiene extraction and it’s the most common of poisons [5]. The ACN concentration in reactant mixture of C_4 or C_5 hydrocarbons is about 100-200 ppm [21]. The main involved reactions of ACN show are: hydrolysis (R13), alcoholysis (with methanol, R14) and Ritter reaction (R15).

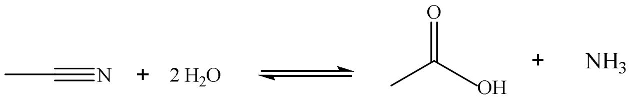

R13

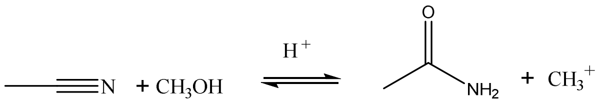

R14

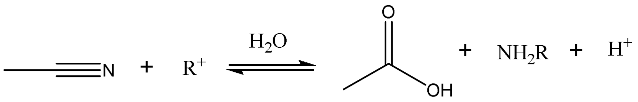

R15

2. OBJECTIVES

Deactivation of ion exchange resins in presence of acetonitrile

2. OBJECTIVES

The aim of this work is to study the catalyst deactivation of Amberlyst ^{TM} 35 and Purolite CT$^{®}$275 by acetonitrile in the simultaneous liquid-phase etherification of isobutene (IB) and isoamylenes (IA) with ethanol using a continuous fixed bed catalytic reactor.

The acquisition of intrinsic kinetic data is an important goal and thus this study has been performed in differential regime (at low conversions) operating in a plug flow reactor at the conditions that assured the absence IMT and EMT effects. Determination of reliable experimental reaction rates and kinetic parameters is an important objective for the modelling of the deactivation process.

Finally, the comparison of the deactivation process over the production of ETBE and TAEE, the evaluation of conversion and selectivity and how they are affected by ACN presence is an important motivation for this work.

3. MATERIALS AND METHODS

Deactivation of ion exchange resins in presence of acetonitrile

3. MATERIALS AND METHODS

The materials, methodology and procedure employed in the experimental runs are described in this chapter.

3.1. MATERIALS

3.1.1. Reactants and Standards

ETBE was synthesized from absolute ethanol (0.1% water, Panreac, Spain) and isobutene (pure, Air Liquide^{TM}). TAEE was synthesized from absolute ethanol (0.1% water, Panreac, Spain) and IA (93.8 wt. % of 2M2B and 6.2 wt. % of 2M1B).Deactivation poison is ACN (99.99%, Fisher Chemical, United Kingdom).

Several standards were employed for the calibration of the system. These consisted as follows; 2-Methyl-2-Propanol or TBA (99.7%, Panreac, Spain); TAA (>98%, TCI, Belgium); Ethanol absolute dry (max. 0.02% water, Panreac, Spain); TAEE (>99.6%) and ETBE (>99.8%) obtained in laboratory and deionized water.

Table 6 shows the most important properties of the mentioned components:

Components	Acronym	ρ [g/mL]	M [g/mol]	Chemical Formula
Water	H_2O	1.000	18.00	H_2O
Acetronitrile	ACN	0.786	41.04	C_2H_3N
Ethanol	EtOH	0.790	46.07	CH_3CH_2OH
Isobutene	IB	0.626	56.00	$(CH_3)_2C=CH_2$
Isoamylenes	IA	0.660	70.14	C_5H_{10}
Tert-butyl alcohol	TBA	0.780	74.12	$(CH_3)_3COH$
Tert-amyl alcohol	TAA	0.810	88.15	$C_5H_{12}O$
Tert-amyl ethyl ether	TAEE	0.770	116.20	$C_2H_5(CH_3)_2COC_2H_5$
Ethyl *tert*-butyl ether	ETBE	0.740	102.18	$(CH_3)_3COC_2H_5$

Table 6. Properties of components employed obtained from sellers.

3.1.2. Tested Catalysts

Two different ion exchange resins have been tested: Amberlyst^{TM} 35 WET (Rohm and Haas France S.A.S.), named as A35, and Purolite CT275 (Purolite SRL), named as CT275. They are solid acid ion-exchange resins with a macroporous structure based on a styrene-divinylbenzene backbone, where sulphonic acid groups, the actual catalytic active centres, are anchored. To build the reactor bed, catalysts were mixed with silicon carbide (silicon carbide powder, coarse, 46 grits, Alfa Aesar, Germany), named SiC, used as the inert.

The chosen catalysts are widely employed in industrial production. Some properties of both catalysts are shown in Table 7. There are two methods to measure pore volume, pore diameter and surface area: ISEC for swollen catalyst and Brunauer-Emmet-Teller method (BET) for dry catalyst.

Properties	**Catalyst A35**	**Catalyst CT275**
Matrix	Macroreticular	Macroreticular
Functional group	$-SO_3H$	$-SO_3H$
Capacity [eq H^+/kg]	5.32	5.2
Max. operating temperature [ºC]	150	145
ρ of bone [g/mL]	1.54	1.51
Total pore volume [mL/g] (BET)	0.210	0.177
Total pore volume [mL/g] (ISEC)	0.736	0.909
Surface area [m^2/g] (BET)	34	21.8
Surface area [m^2/g] (ISEC)	165.7	182.8
Average pore diameter [Aº] (BET)	236	329
Average pore diameter [Aº] (ISEC)	150	199
Porosity [%] (BET)	24.5	21
Porosity [%] (ISEC)	52.3	61.3

Table 7. Physical and structural properties of A35 and CT275.

Used Dp (with sieving) is within the range 0.25-0.4 mm. Previous studies confirmed the absence of IMT using these bead size [20].

3.1.3. Experimental Setup

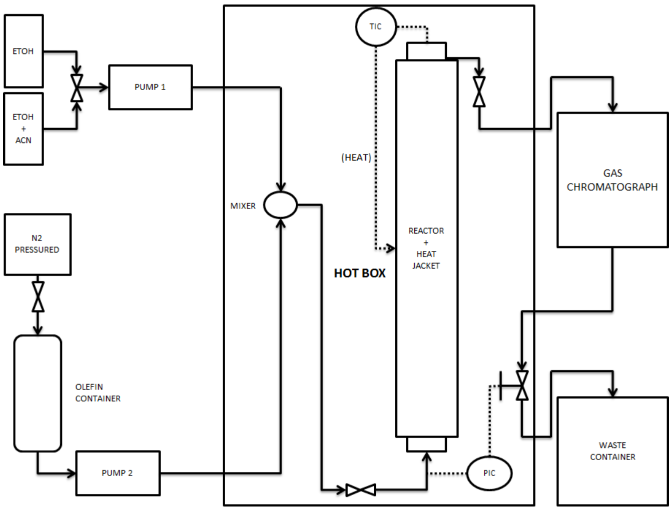

Figure 15. Scheme of experimental setup.

Pump 1 pumped pure ethanol and contaminated ethanol depending on the position of the three-ways valve. Pump 2 pumped the olefin mixture from the pressurized container. Both streams are mix in the mixer, inside the hot box. After the pumps two check valves are placed to prevent fluid back. The temperature indicator controller (TIC) was a thermocouple (indicator) situated in bed zone and a heat jacket (controller) around the reactor. The pressure indicator controller (PIC) measured the pressure in reactor inlet and acted by a valve situated after the chromatograph, to ensure liquid-phase along the setup pipelines.

3.1.4. Apparatus and Analysis

Experiments were carried out in a stainless steel tubular continuous fixed bed reactor as is illustrated in Figure 16.

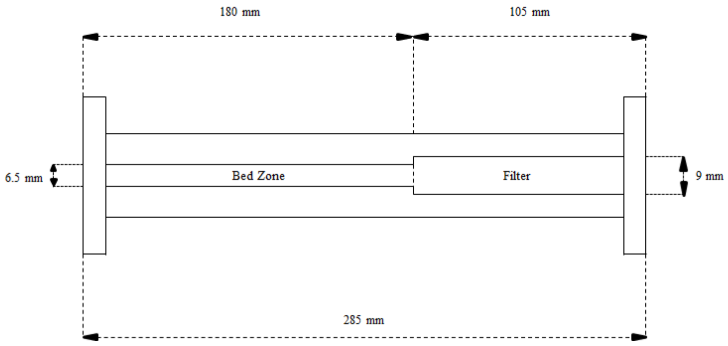

Figure 16. Diagram of the reactor measures. Blue arrow indicates the flow direction.

The flow direction indicated in Figure 16 implies ascendant flow when reactor is connected in the system. The bed zone is the real reactor zone, rest of reactor consists in a filter (with a length of 10.5 cm) to fix the catalytic bed and to avoid the entrance of catalyst particles to the rest of parts of the experimental setup: there is a filter in the reactor outlet too. Useful length is about 18 cm and implies a useful reactor volume of 6 mL. The catalytic bed consists of a mixture of catalyst and SiC particles with the range of same particle size. This is an important condition, because to operate in the differential regime (conversion lower than 10%), the catalyst load must be low and accurately adjusted. Reactor is equipped with one thermocouple in bed zone to control the temperature: this thermocouple is placed at reactor outlet.

A picture of reactor is shown in Figure 17.

Figure 17. Stainless steel tubular reactor. Frontal and lateral view.

The experiments were carried out in Microactivity-Reference reactor (Process Integral Development Eng&Tech S.L., Madrid, Spain). The panel control of the software employed is shown in Figure 18.

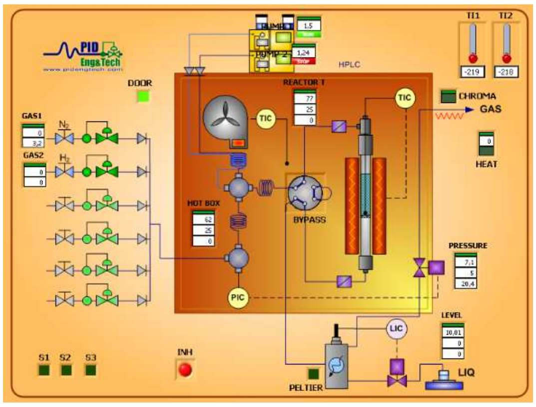

Figure 18. Panel Control of Microactivity-Reference reactor.

Microactivity-Reference reactor has a proportional-integral-derivative (PID) controller for pressure and temperature (of reactor and hot box). The reactor temperature is measured (TI) by thermocouple placed in the catalytic bed and is controlled (TC) by the heat jacket. The hot box temperature is controlled by a forced convection electric heater. The system pressure is controlled by a stainless steel valve (Hoke, model 1315G2Y, with a maximum operating pressure of 345 bars at 21ºC) with a control accuracy of ±0.1 bar, situated after the gas-chromatograph.

In order to control the process variables P and T, correct values for the parameters P (proportional), I (Integral) and D (derivative) were estimated. These values are shown in Table 8.

Control parameter	P	I	D
Pressure of system	50	50	0
Reactor temperature	60	400	60
Hot box temperature	16	120	20

Table 8. Values of PID for a correct control of system process variables.

Figure 19 shows parameters evolution from initial value until set value: is observed that parameters are stabilized in more or less half an hour. Figure 20 shows the actuation of control elements.

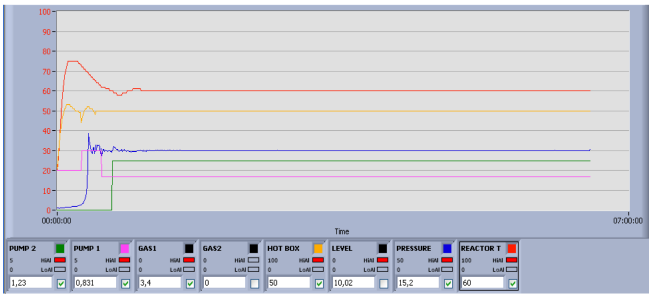

Figure 19. Process Values diagram

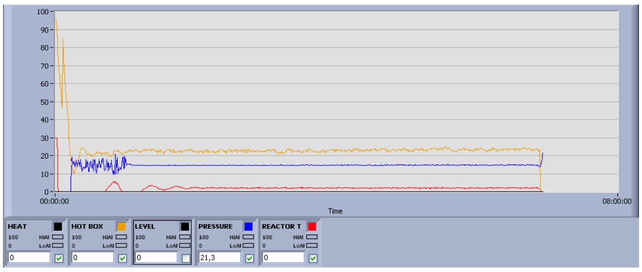

Figure 20. Output Controller diagram

Samples of 0.2 µL of liquid reaction medium were taken on-line from the reactor outlet with a valve (Valco A2CI4WE.2, VICI AG International, Schenkon, Switzerland). The composition was determined in an HP6890A GLC (Hewlett Packard) equipped with thermos-coupler detector (TCD). A cross-linked methyl silicone, 50m x 0.2mm x 0.5µm capillary column HP-Pona (Agilent Technologies, 6890N Network GC System) was used to separate and quantify the compounds present in the reaction mixture. Column use helium (>99.998%, Linde) as carrier gas. An example of the chromatographic analysis obtained is illustrated in Figure 21, where the different set of peaks correspond to repetitive injection of samples. Chromatograph inlet is connected with the outlet-stream of the reactor.

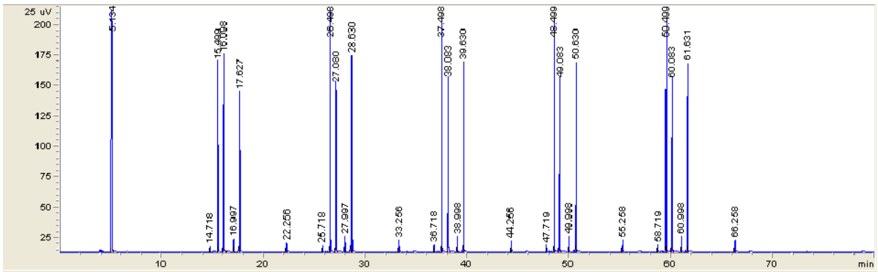

Figure 21. Picture analysis of chromatograph

Other important elements of the experimental setup are the two HPLC pumps (pump 307, Gilson, with a precision of 0.001 mL/min). One is connected to a glass vessel with ethanol (pure or contaminated ethanol) and the other is connected to a stainless steel cylinder that contains the mixture of olefins (isoamylenes and isobutene).

The last relevant elements in the experimental setup are the containers for reactants. On one hand there are two glass-vessels (one for pure ethanol and other for ethanol with ACN) and on the other hand, there is a stainless steel cylinder to contain liquid at high pressure. The switch to change between pure and poisoned ethanol consists in a three-ways valve. The feed-stream of olefins is pressurized with nitrogen (to assure the liquid phase of the olefins mixture).

Along the experimental setup there are filters to avoid the presence of small particles.

3.2. EXPERIMENTAL METHODS

3.2.1. Operating Conditions

ETBE and TAEE reactions present high conversion and selectivity in a wide range of temperatures (from 40ºC to 80ºC [5]). For this reason industrial units operate within this range of temperature. The temperature was varied in the mentioned range, from 40 to 80ºC, with an instrumental error of ±0.1 ºC. At these temperatures, pressure was set to 15 bars to ensure liquid-phase of components. The selected ethanol/olefins molar ratio was $R_{EtOH \rightarrow OLEFINS} = 1.1$ to avoid oligomerization reactions with a slight excess of ethanol, and molar ratio IA/IB was fixed in 1 ($R_{IA \rightarrow IB} = R_{IB \rightarrow IA} = 1$). Volumetric flow was set to fulfil the molar ratio between alcohol and olefins, as it is shown in Table 9.

Pump	Components	Volumetric flow [mL/min]
Pump 1	EtOH/EtOH+ACN	0.831±0.001
Pump 2	IB+IA	1.23±0.001

Table 9. Volumetric flow for pumps

ACN concentration in contaminated ethanol was varied from 500 ppm to 4000 ppm. Water effect was also studied and varied from 0 ppm (minimum water content in dry ethanol) to 4000 ppm. All experimental conditions are described in Annex 1.

3.2.2. Catalyst: pretreatment and use.

The catalyst must be pre-treated before be loaded into the reactor. Firstly, the catalyst is grinded and sieved to obtain the desired range of particle size (0.25-0.40 mm)

[20]. In the second part, the catalyst was dried in order to avoid uncontrolled source of water within the system. The catalyst was dried for 2.5 hours in an atmospheric oven 110ºC and subsequently 15 h in a vacuum oven at the same temperature. The remaining water content obtained using such procedure is about 3.5 wt% (results extracted of previous studies [9]).

Only differential experiments were performed in this work. The catalyst amount was fixed in small values to ensure a conversion lower than 10% for all reactants but big enough to accomplish catalyst diffusion ratio (DR). DR (Equation 7) was demonstrated that presents problems for values higher than 300 [16].

$$DR = \frac{M_{inert}}{M_C} < 300 \qquad \text{Equation 7}$$

The amount of catalyst used for each experiment depends on temperature: larger catalyst loads were used at lower temperature. The reason to do it is for obtaining significant ethers production assuring differential regime (low conversions). Table 10 shows the loads of catalyst used at each working temperature and DR in each temperature level. The amount of silicon carbide-inert depends on the reactor free volume and must be calculated previously employing densities of catalysts and SiC. The same amount of catalyst was employed to compare the catalytic activity decay of A35 and CT275.

M_C[g]	M_{inert}[g]	DR<300	$T_{REACTION}$[ºC]
1	8.5	8.50	40
0.16	11.4	71.25	60
0.04	11.5	287.5	80

Table 10. Catalyst amount as a function of temperature.

3.2.3. Fluid Dynamics

Experiments are carried out under plug flow conditions. Two conditions (Equation 8 and 9) must be fulfilled to assure plug flow, that is, to reduce axial dispersion effects and to reduce the wall effects, respectively:

$$\frac{\mathrm{L}}{\mathrm{Dp}} > 100 \qquad \text{Equation 8}$$

$$\frac{\mathrm{D}}{\mathrm{Dp}} > 10 \qquad \text{Equation 9}$$

To ensure it, the larger Dp was chosen (0.40 mm) to check the conditions: L/Dp = 437.5 > 100 and D/Dp = 16.25 > 10. Both conditions are fulfilled and plug flow can be therefore assured.

3.2.4. Chromatographic Analysis Conditions

The chosen program presents a constant oven temperature of 35 ºC; a helium flow of 1 [mL/min]; an average velocity inside column of 25 [cm/s] and a split ratio of 1/75.

In this study was employed a program of 80 minutes comprising six overlapped analyses. This imply a new sample every 11 min. The duration of each individual analysis was about 25 min (TAEE is the component with the highest elution time at 23.45 min). The chromatographic program can be varied to reduce program duration if is expected achieving stationary state soon, for example.

The first elution or retention time (RT) for each component is shown in Table 11.

Components	RT_1[min]
H_2O	4.0
IB	4.5
EtOH	5.1
ACN	5.2
2M1B	5.9
TBA	6.4
2M2B	6.6
ETBE	11.3
TAA	11.8
TAEE	23.8

Table 11. RT for all components.

3.2.5. Calibration

Chromatograph calibration consists in the preparation of mixtures of known composition. These mixtures are analysed in chromatograph. Each composition is assigned to a chromatographic area. Finally, a calibration curve is obtained that relates composition and chromatographic area for each chemical compound. Tables with all calibrated composition and graphs with curves obtained are illustrated in Annex 2. The calibration procedure is different for each pump and is described below.

For pump 1, the calibration was realized by direct method: pumping a known amount of ethanol (ethanol pumped was weighed) in a known time. These data was represented, and the slope between volume (obtained by ethanol density) and time pumping is the volumetric real flow. These data obtained are in Annex 3.

For pump 2, the calibration was realized by inverse method. This consists in the measure of the loss weigh of a high pressure container loaded with the mixture IA/IB at different times. This calibration had to be doing thus because IA and IB are very volatile compounds, and this characteristic manipulates the direct method results. The drawback of this method is the low precision of weighing scales employed in order to allow weigh the big weight of high pressure container. These data are in Annex 3.

The main conclusion of both pumps calibrations is that volumetric flow indicated in pumps panel may be considered as accurate since the differences between nominal and real values are very small. The curves, results and calibration procedure are in Annex 3.

3.2.6. Experimental Procedure

All steps that must be followed to perform an experiment are listed below:

Step 1: Pretreatment of the catalyst.

Step 2: Set up the reactor and load the catalyst.

Step 3: Fix the reactor to the heat jacket and connect to system of piping within the hot box.

Step 4: Prepare the desired ethanol contaminated with ACN and/or water and fill the corresponding containers.

Step 5: Make hydraulic priming with a syringe as is indicated in “307 Piston Pump User’s Guide”. This is essential to prevent a drop of gas into the pump head because severe damage can result.

Step 6: Start “MICROACTIVITY reference” and start the software of the chromatograph.

Step 7: Firstly, only “pure” ethanol was fed to the system until the pressure and temperature reached the set values. Once system values are stabilized is time to start olefins’ feed.

Step 8: The obtained chromatographic analysis are evaluated in line to determine when stationary state is reached. The steady state is always reached with pure ethanol to determine the reaction rate in the absence of deactivating agent, and, afterwards, the ethanol feed stream was switched (by means of the three way valve) to the ethanol-poison mixture in order to start the deactivation experiment. The duration of deactivation experiments time was about 4 hours for all the runs.

Step 9: When that time is up, pump 2 is turned off. This time must be considered to obtain (knowing the volumetric flow) the remaining amount of olefins inside the steel cylinder.

Step 10: Change the position of three-way valve. Pump 1 must continue operating about 30 min to clean the system of remaining ACN.

Step 11: Set PID values for temperature of hot box and reactor to return to environment value. Finally, the pressure must be fixed at 1bar. Then, the system may be turned off.

3.2.7. Experimental Calculations

Outlet reactor composition (expressed in mass fractions) is obtained from chromatograph area with graphs of calibration. The composition summation must be equal to 100% (Equation 10), within the experimental error, for the summation of the *n* components present in reaction system.

$$\sum_{i=1}^{n} \%m_i = 100$$ Equation 10

Experimental composition summation obtained usually presented values between 95-98%, due to the experimental error. To minimize its effect, the relative composition with respect 2M2B was considered, following Equation 11.

$$\sum_{i=1}^{n} \frac{\%m_i}{\%m_{2M2B}} = \frac{100}{\%m_{2M2B}}$$ Equation 11

Normalized value for each component is obtained by Equation 12.

$$\%m_i^{norm} = \left(\frac{m_i}{m_{2M2B}}\right) \cdot \left(\frac{100}{\sum_{i=1}^{n} \frac{\%m_i}{\%m_{2M2B}}}\right)$$ Equation 12

In this point, reactor outlet stream is obtained. Reaction rate is obtained following Equation 13 for products (*j*) and Equation 14 for reactants (*i*).

$$r_j = \frac{F_j^{outlet}}{M_C}$$ Equation 13

$$-r_i = \frac{F_i^{inlet} - F_i^{outlet}}{M_C}$$ Equation 14

Conversion is obtained by Equation 15 for each reactant.

$$X_j = \left(\frac{F_j^{inlet} - F_j^{outlet}}{F_j^{inlet}}\right) \cdot 100$$ Equation 15

Conversion (X) can be expressed by other way: from products outlet stream. Then, conversion of IB, for example, can be formulated by Equation 16.

$$X_{IB} = \left(\frac{F_{ETBE}^{outlet} + F_{TBA}^{outlet}}{F_{IB}^{inlet}}\right) \cdot 100 \qquad \text{Equation 16}$$

Selectivity (S) was also studied. Equation 17 illustrates the general form to calculate selectivity.

$$S_i^j = \frac{mole\ of\ i\ reacted\ to\ form\ j}{total\ mole\ of\ i\ reacted} \cdot 100 \qquad \text{Equation 17}$$

There were three main reactants in studied system. These can form different byproducts, but with the operating conditions selected the selectivity to form ether was always of 100% or very near (TBA appeared at low amount in some experiments; TAA only appeared in one experiment with much amount of initial water). Ethanol was only considered that produced ETBE and TAEE, not minority byproducts as DEE which didn't appear in chromatograph analysis. Then, ethanol selectivity only was studied between ETBE and TAEE. IB selectivity was studied considering TBA and ETBE production. IA selectivity wasn't studied because was considered that only produced TAEE.

The selectivities of ethanol to both ethers were calculated following Equations 18 (for selectivity to ETBE or TAEE). Selectivity can be expressed from reaction rate or molar outlet stream (considering stoichiometry relationship).

$$S_{EtOH}^{ETBE/TAEE} = \frac{r_{ETBE/TAEE}}{r_{ETBE} + r_{TAEE}} \cdot 100 = \frac{F_{ETBE/TAEE}^{outlet}}{F_{ETBE}^{outlet} + F_{TAEE}^{outlet}} \cdot 100 \qquad \text{Equation 18}$$

The IB selectivities (to ETBE or TBA) were calculated following Equation 19

$$S_{IB}^{ETBE/TBA} = \frac{r_{ETBE/TBA}}{r_{ETBE} + r_{TBA}} \cdot 100 = \frac{F_{ETBE/TBA}^{outlet}}{F_{ETBE}^{outlet} + F_{TBA}^{outlet}} \cdot 100 \qquad \text{Equation 19}$$

Deactivation of ion exchange resins in presence of acetonitrile

4. RESULTS AND DISCUSSION

4 RESULTS AND DISCUSSION

Catalytic activity level at each instant can be estimated as the ratio between reaction rate of compound *j* at time *t* and reaction rate for the same compound at the steady state in the absence of the deactivating agent, which was assigned to time zero. Activity is dimensionless and is described by Equation 20.

$$a_j^t = \frac{r_j^t}{r_j^0} \qquad \text{Equation 20}$$

4.1. Reaction Rate

Experimental reaction rate data are presented in this section. An example of the reaction rate profile obtained during an experimental run is presented in Figure 22 and 23 each for different experimental conditions. In these graphs the reaction rates, expressed as $[\frac{mol}{kg\ cat \cdot h}]$, are the y-axis while time on stream (TOS), expressed in minutes, is the x-axis. These data allow a comparison between reaction rates of both etherification reactions (TAEE and ETBE productions).

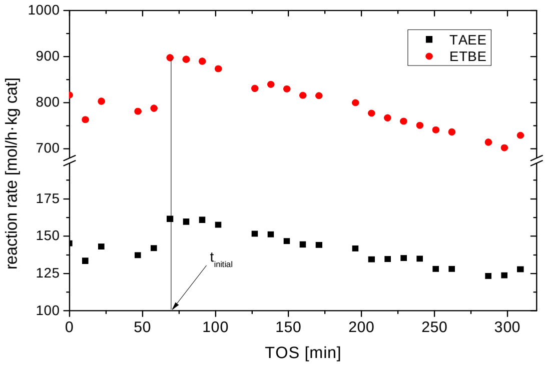

Figure 22. A-35; T=80ºC; [ACN]=500 ppm.

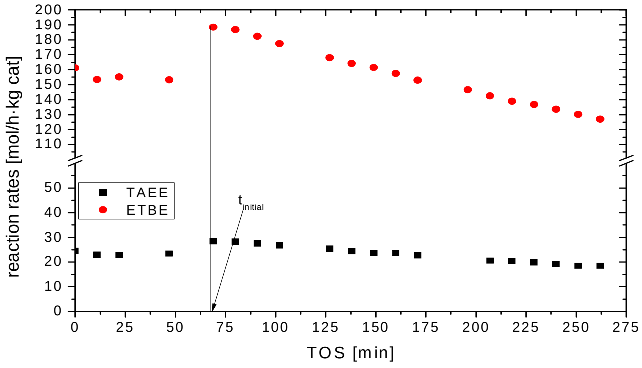

Figure 23. A-35; T=60ºC; [ACN] = 3100 ppm.

Reaction rates of ETBE are remarkably higher than reaction rates of TAEE for the same temperature. Then some conclusions are expected: selectivity of ethanol to ETBE is higher than selectivity to TAEE.

Obviously, at higher temperature, obtained reaction rates increased for both ETBE and TAEE, since kinetic constants of formation reactions of both ethers are expected to follow the Arrhenius Law.

Initial time, named $t_{initial}$ in the graphs, has been taken as the instant at which the ACN effect is detected in the chromatographic analysis. The delay with respect time zero is due to the time needed to the reactants to flow from the ACN feed until the sampling valve.

Initially, a reaction rate increase with respect to the stationary value is observed, what can be attributed to the reaction of water with ACN and/or by replacement of adsorbed water on the resin by ACN. Initially, adsorbed water can be occupying three active centres as is shown in Figure 24.

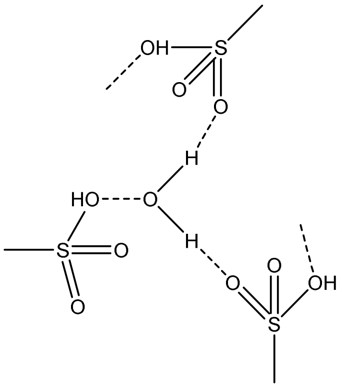

Figure 24. Representative structure of one water molecule hydrogen-bonded to three undissociated –SO_3H groups [12].

Water acts as inhibitor. As ACN enters into the resin, two mole of water can react with one mole of ACN (R13). Then, water molar disappearance is faster than ACN and this last one begins to form ammonia, which is the actual deactivating agent for the resin. Once it occurs, reaction rate begins to decrease by neutralization of active centres (Figure 12). Furthermore, the high affinity of ACN molecules to dissociated acids groups (by the basic character of ACN) can replace water molecules of the active centres. ACN is aprotic polar dissolvent and not form hydrogen-bonds [22]. Then, active centres could be released when water is replaced or reacts.

4.2. Effect of ACN concentration

Different experiments were carried out, where ACN concentration ([ACN]) in the fed ethanol was varied from 500 to 4000 ppm to quantify its effect on the deactivation progress, see Figure 25. Tested [ACN] are higher than typical values in industrial unit but were necessary to acquire data in a reasonable reaction time. Results are plotted in terms of activity for y-axis and TOS for x-axis. Henceforward, the catalyst deactivation usually will be shown in terms of activity instead of reaction rate values, for the shake of clarity in comparing deactivation progress under different conditions.

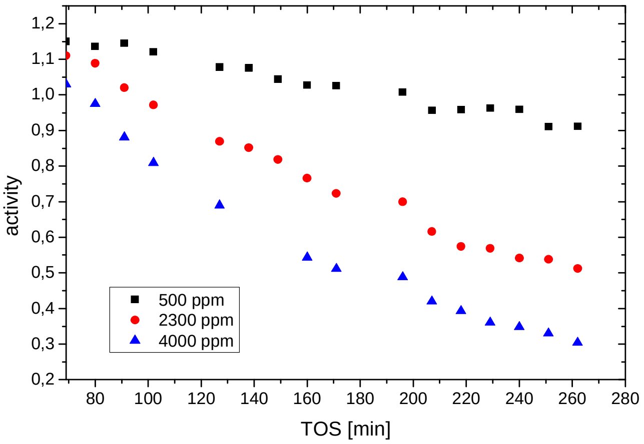

Figure 25. TAEE's activity decay with different [ACN] at 80ºC employing A35.

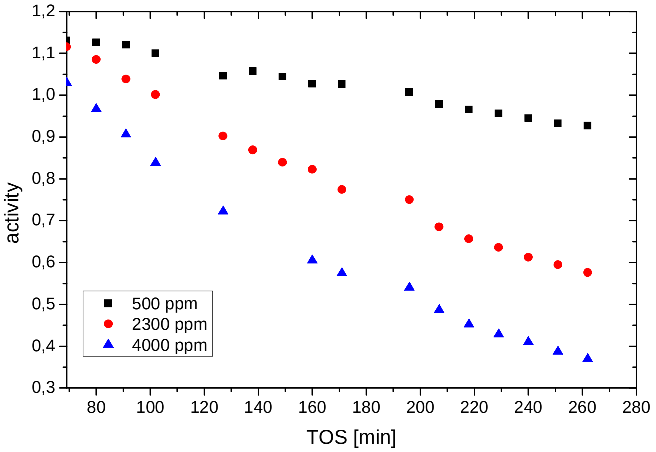

Figure 26 ETBE's activity decay with different [ACN] at 80ºC employing A35.

Activity decay was enhanced by higher concentration of poison. This demonstrates direct relationship between decay of activity and [ACN], as expected.

Although at low [ACN] deactivation progress can be considered as lineal with time, at high [ACN] this progress approaches to an Exponential-type curve

Activity decay rate was higher for high values of [ACN] at initial times, but at last times activity decay curve approached to a horizontal asymptote. Activity decay rate decreased with time.

The plotted results can be compared with values of other study [20] only for the case of T = 80ºC; [ACN] = 500 ppm and $R_{EtOH\rightarrow olefins}$=1.1 (other conditions weren't the same between the other work and this work). More deactivation effect was observed in other study under the same conditions. Furthermore the initial activity increase didn't appear in other study. The reason of this difference among both studies is the employed ethanol: other study employed more dried ethanol. Even so the trends of graphs were the same in both studies.

4.3. Effect of deactivation on ETBE and TAEE formation

ACN affects both etherifications. Figure 27 and 28 show deactivation effect on TAEE and ETBE production and it allows to compare between both syntheses.

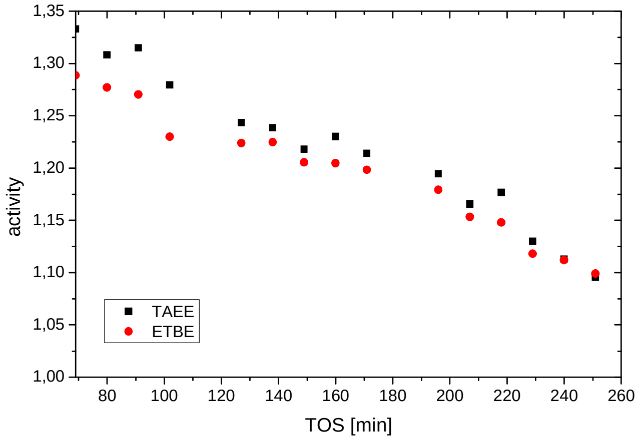

Figure 27. Activity decay of A35 at 60ºC with [ACN] = 1100 ppm.

Figure 27 was similar for both ethers, higher for TAEE or ETBE depending the experiment.

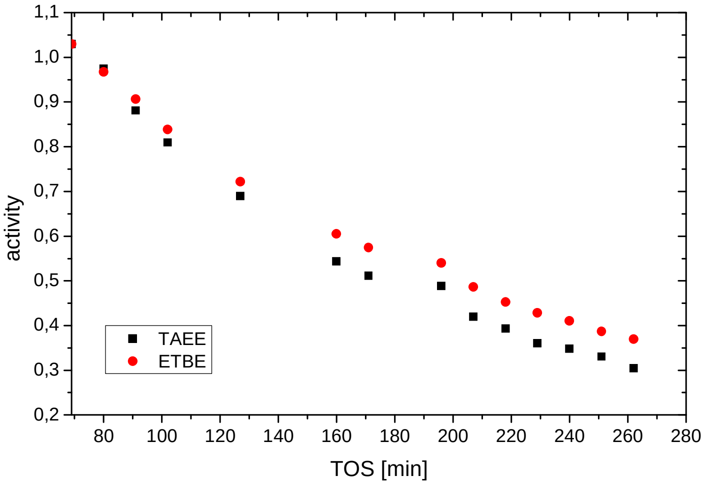

Figure 28. Activity decay of A35 at 80ºC with [ACN] = 4000 ppm

The deactivation effect of ACN was more important for TAEE than for ETBE as can be observed Figure 27 and 28, where activity decay rate was higher for TAEE than for ETBE. Then ACN affected in different way to ETBE or TAEE. The reason may be due to the larger molecular size of TAEE than ETBE. Active centres were more inaccessible for IA than for IB when ACN deactivation began.

Activity decay seems lineal-type in Figure 27 whereas seems exponential-type in Figure 28, but could be by effect of temperature or poison concentration.

4.4. Effect of Temperature

Figures 29 and 30 show the effect of different temperature with the same [ACN] (4000 ppm) and water content (0 ppm) for TAEE or ETBE.

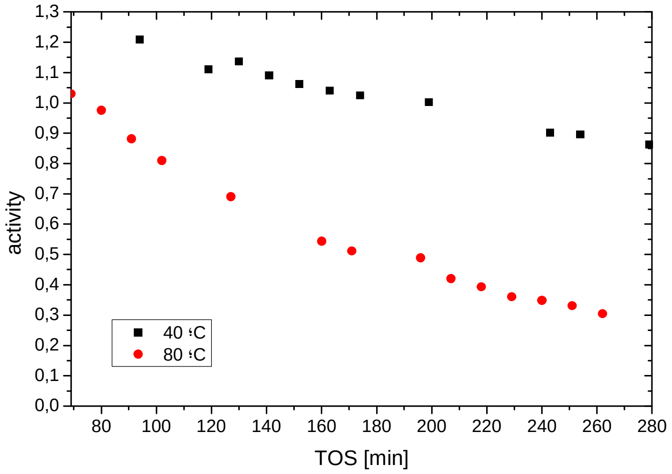

Figure 29. TAEE’s activity decay at different temperatures with [ACN] = 4000 ppm.

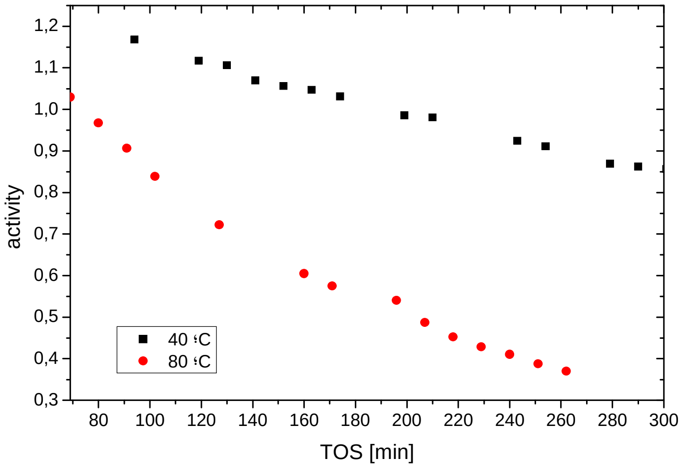

Figure 30. ETBE’s activity decay at different temperatures with [ACN] = 4000 ppm.

As it can be seen in Figure 29 and 30 the higher temperature increased, the higher the deactivation effect. On the other hand, low temperatures imply slower deactivation rates and therefore longer catalyst lifespan. This fact does not imply that low temperatures are more interesting.

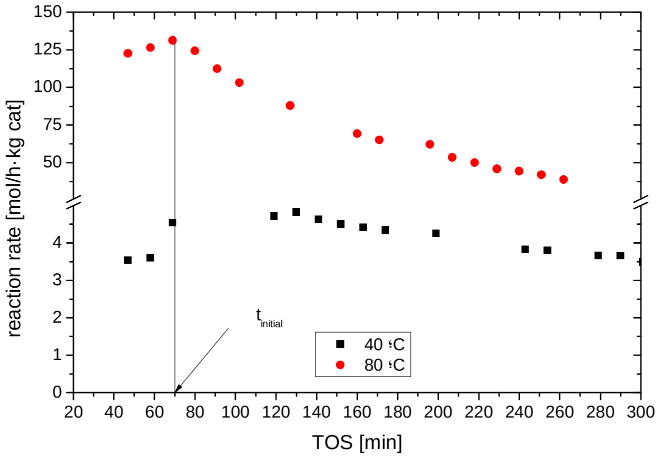

Figure 31. TAEE’s reaction rate decay at different temperatures with [ACN] = 4000 ppm.

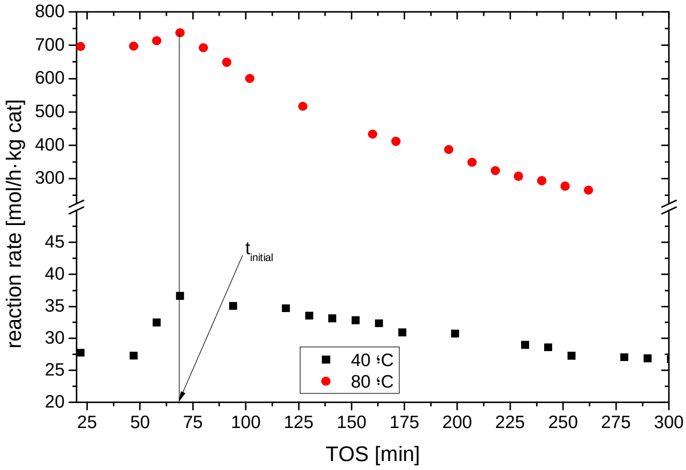

Figure 32. ETBE's reaction rate decay at different temperatures with [ACN] = 4000 ppm.

4.5. Catalyst Effect

Two different types of catalysts were studied in this project: A35 (the main studied catalyst) and CT275 (only was employed in one experiment for comparison purposes).

Activity decay is shown in Figures 33 and 34 under the same operating conditions (T = 60 ºC and [ACN] = 3100 ppm)

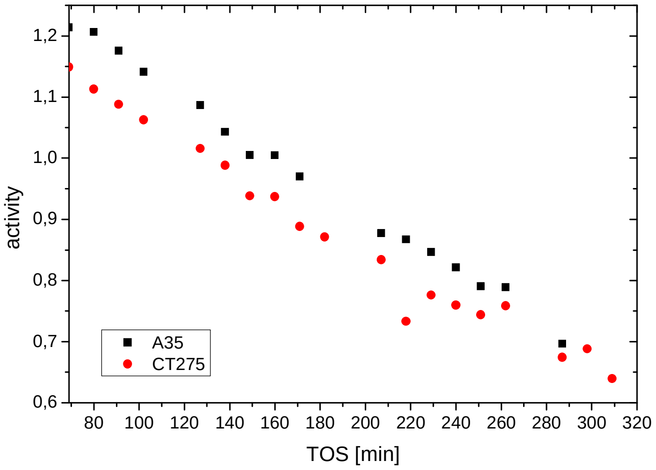

Figure 33. Activity of TAEE at T = 60ºC and [ACN] = 3100 ppm.

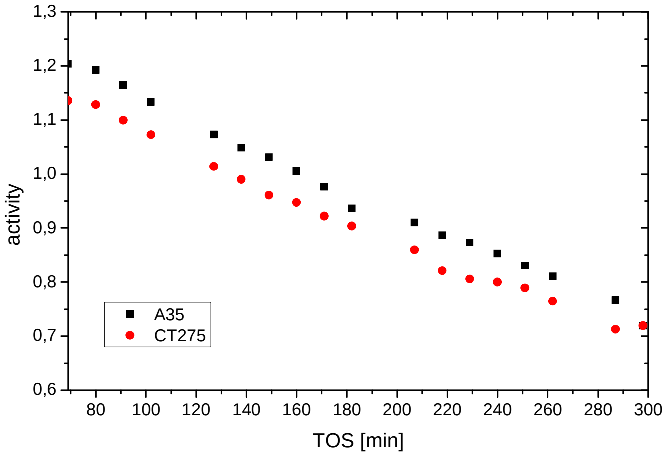

Figure 34. Activity of ETBE at T = 60ºC and [ACN] = 3100 ppm.

Activity decays are similar in both cases. Maximum value of activity with catalyst A35 is higher than maximum value of activity with CT275, but rate of deactivation is slightly higher for A35 than for CT275: both catalysts start in different values but end in similar values after 300 min. This could be due to the different average pore diameter of both catalysts: it is larger for CT275 than for A35 (Table 7). When ACN deactivation began, active centres unneutralized of CT275 was more accessible than active centres unneutralized of A35. Then, CT275 is more resistant at ACN deactivation.

Figure 35 and 36 show reaction rates under the same conditions than Figures 33 and 34.

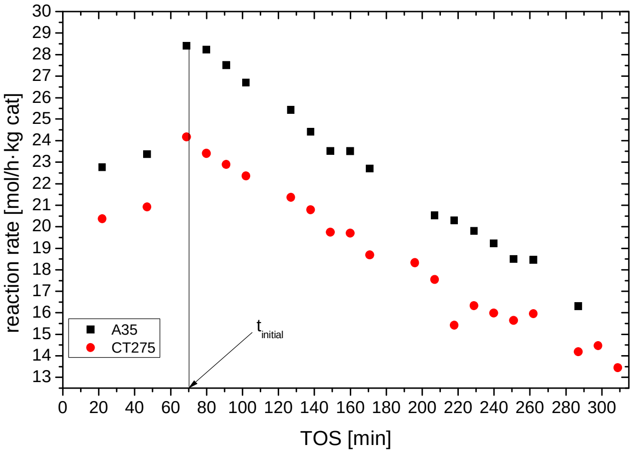

Figure 35. Reaction rates for TAEE at T = 60ºC and [ACN] = 3100 ppm.

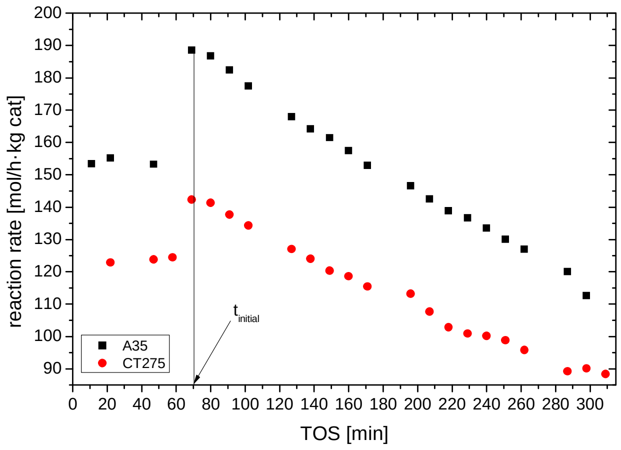

Figure 36. Reaction rates for ETBE at T = 60ºC and [ACN] = 3100 ppm.

Catalyst A35 offers better performance under the same operational conditions (reaction rates in stationary state is higher). This is due to the higher acid capacity (Table 7) and acid site density [5] of A35 than CT275.

4.6. Effect of Water

Figures 37 and 38 plot the experimental activity decay for different concentration of water ([H_2O]) in the ethanol feed stream.

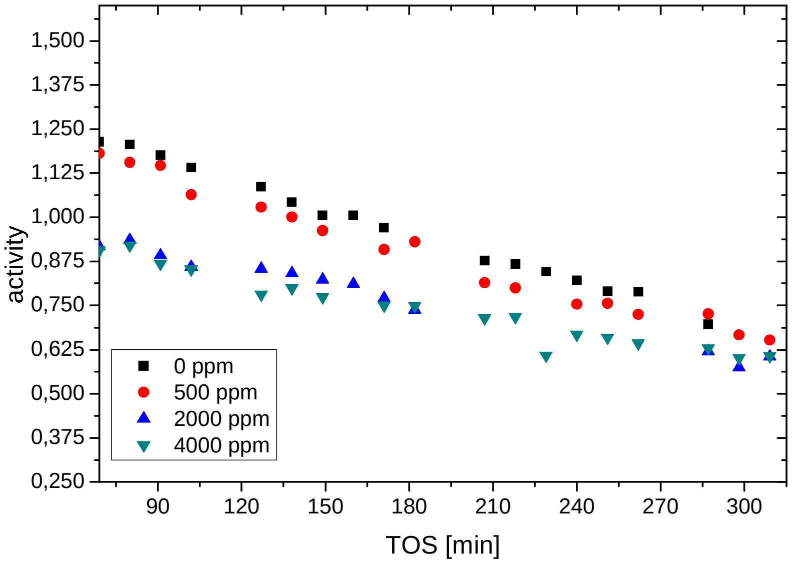

Figure 37. Effect of water in TAEE deactivation at T = 60ºC and [ACN] = 3100 ppm.

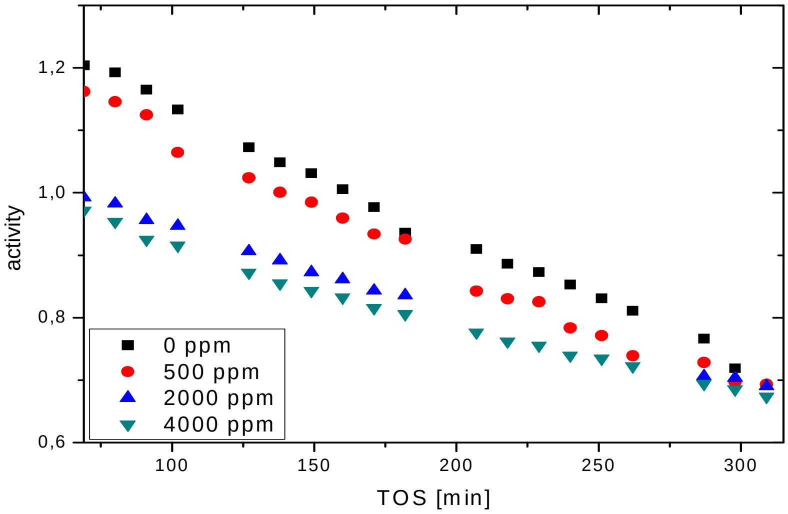

Figure 38. Effect of water in ETBE deactivation at T = 60ºC and [ACN] = 3100 ppm.

The effect of initial water presence is observed in Figures 37 and 38. At more amount of water in ethanol, the initial maximum value of activity decreased but posterior activity decay rate decreased too. Water presence worsens ACN deactivation

Water acts also as inhibitor as can be observed in values of reaction rate. Figures 39 and 40 plot these values.

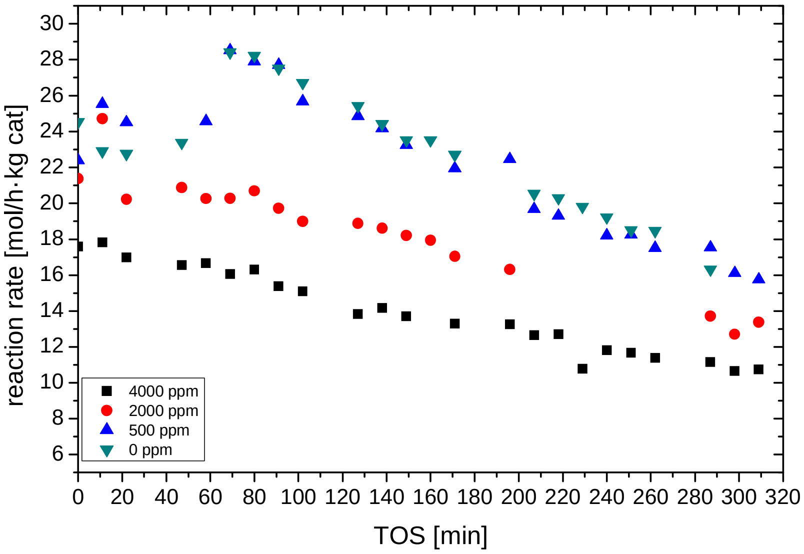

Figure 39. Effect of water in TAEE reaction rate decrease at T = 60ºC and [ACN] = 3100 ppm.

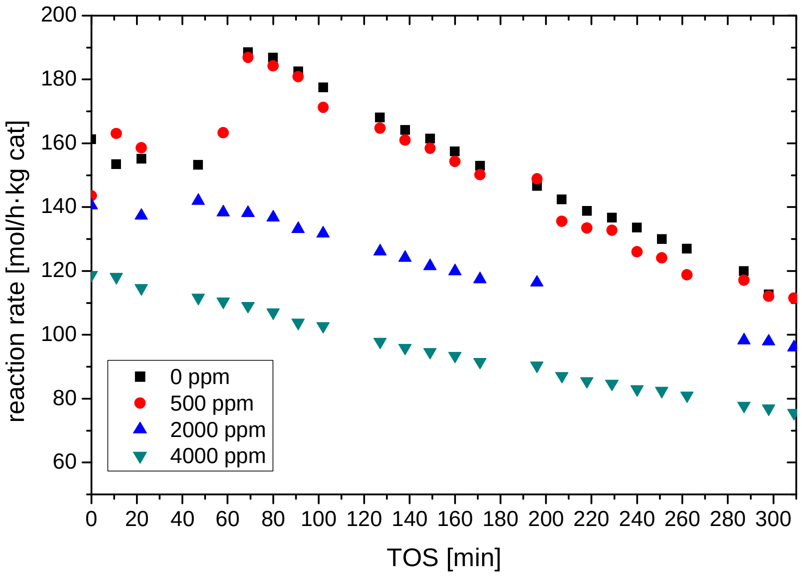

Figure 40. Effect of water in ETBE reaction rate decrease at T = 60ºC and [ACN] = 3100 ppm.

Figures 39 and 40 show a direct relationship: with more initial water amount, less reaction rate for both ether productions. These graphs confirm that water acted as inhibitor of studied reactions.

4.7. Activation Energy

The steady state reached in each experiment before feeding ACN to the reactor allowed the estimation of apparent activation energy values for the involved etherification reactions. Assuming a potential model, kinetic equations can be fit to experimental data as described below (for the case of ETBE).

$$r_{ETBE} = k\, C_{EtOH}^{X} C_{IB}^{Y} \qquad \text{Equation 21}$$

The kinetic constant is described by Arrhenius Law (Equation 22). The exponent X (of EtOH concentration) and exponent Y (of IB concentration for ETBE and IA concentration for TAEE) were obtained showing a zero order for the alcohol concentration and positive order (one) with respect to the olefin concentration. The fit, calculations and obtained values of exponents are shown in Annex 4.

$$k = A \exp\left(\frac{-E_{act}}{R\,T}\right) \qquad \text{Equation 22}$$

By considering that reactants concentration are the same, a new constant B can be defined as:

$$B = A\, C_{ETOH}^{X} C_{IB}^{Y} \qquad \text{Equation 23}$$

The kinetic equation can be reordered and expressed by Equation 24.

$$r = B \exp\left(\frac{-E_{act}}{R\,T}\right) \qquad \text{Equation 24}$$

And if Equation 24 is linearized:

$$\ln r = \ln B - \left(\frac{E_{act}}{R}\right)\frac{1}{T} \qquad \text{Equation 25}$$

Therefore, ln r_i versus 1/T should be a straight line that can be described by linear regression. The slope of the resulting straight line is ($-E_{act}/R$). An example (for T=60ºC) of the procedure for obtain the considered points plotted in Figure 41 is shown in Table 12.

Experiment	r_{ETBE} [mol/(h·kg cat)]	r_{TAEE} [mol/(h·kg cat)]
E3	150.1	21.9
E5	156.6	23.4
AVERAGE	**153.3 ±4.65**	**22.6 ±1.05**

Table 12. Example of calculation of stationary reaction rate at 60ºC

T [K]	r_{TAEE}[mol/h·kg cat]	ln r_{TAEE}	r_{ETBE}[mol/h·kg cat]	ln r_{ETBE}	1/T [K^{-1}]
313.14	4.2±0.01	1.45±0.0047	31.3±0.15	3.45±0.0066	0.0032
333.14	22.6±1.05	3.12±0.062	153.3±4.65	5.03±0.035	0.0030
353.14	134.0±8.7	4.90±0.092	754.6±47.8	6.63±0.089	0.0028

Table 13. Values obtained for graphical representation.

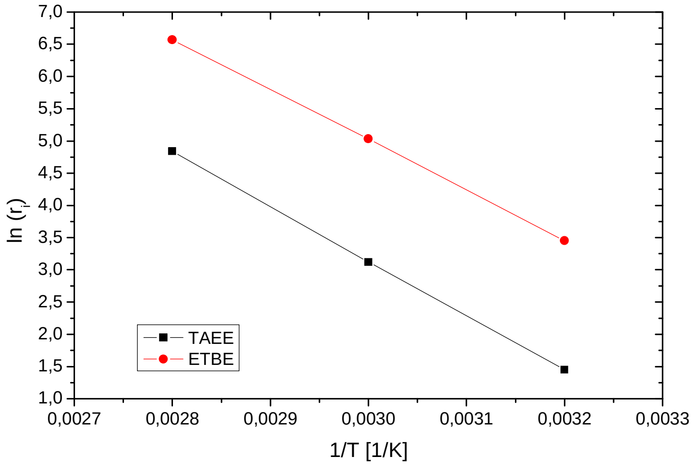

Figure 41. Arrhenius plot for both ETBE and TAEE synthesis.

Element	R^2	$-E_{act}/R$ [K]	E_{act} [KJ/mol]
ETBE	0.9991	-8784.9	73.0 ±3.0
TAEE	0.9979	-9528.7	79.2 ±10.7

Table 14. Obtaining of the energy of activation (R=8.31 [J/(K·mol)]).

Similar results were obtained in previous studies [23]. Table 15 shows the comparative between values. The values of activation energy were also obtained optimizing by Solver and are shown in Annex 4.

	E_{act} [KJ/mol]	
Ether	**This project**	**Literature**
ETBE	73.0 ±3.0	77.5 ±11.0
TAEE	79.2 ±10.7	86.3 ±8.8

Table 15. Activation Energy of both studies.

Some values of reaction rate obtained and showed in Table 13 can be compared with values of previous study [5, 14,24] under similar conditions. Table 16 compares these values.

		Reaction rate [mol/(h·kg$_{cat}$)]	
T [ºC]	**Ether**	**This project**	**Literature**
80	ETBE	754.6	797 [14]
60	ETBE	154.6	180 [5]
60	TAEE	22.6	100 [24]

Table 16. Stationary reaction rate at T=80ºC with $R_{EtOh \rightarrow olefins}$=1.1.

The value obtained in this work with two simultaneous etherifications was lower than that obtained for the individual synthesis of ETBE in previous studies. The value of reaction rate for TAEE is obtained from a graph and is approximated. However it is clear that reaction rate of TAEE individual production is higher than simultaneous etherification. The explanation may be due to two factors: a dilution of the reactants and the use of ethanol with higher water content.

4.8. Effect on Selectivity

Figures 42 and 43 show selectivity of ethanol at different temperatures.

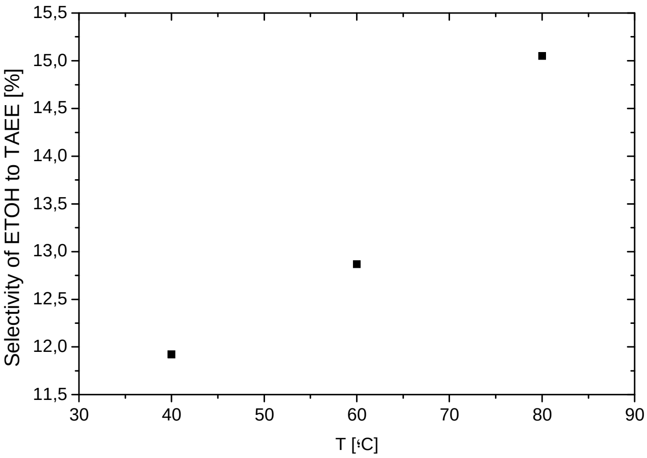

Figure 42. Selectivity of ethanol to TAEE.

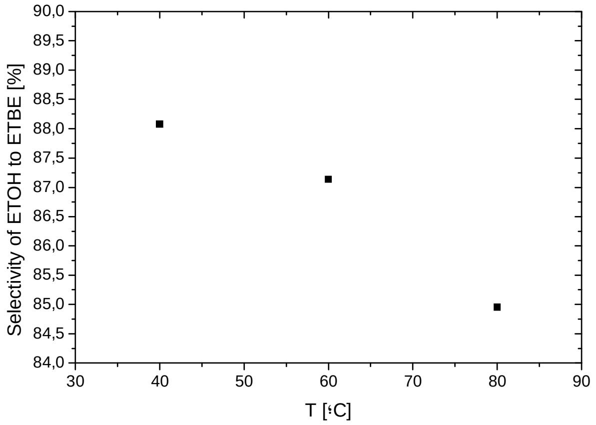

Figure 43. Selectivity of ethanol to ETBE.

Selectivity of ethanol to TAEE increased as the temperature is higher. EtOH selectivity toward ETBE formation followed an opposite trend. Then, TAEE reaction was more enhanced with temperature than ETBE reaction.

The values of selectivity between both catalysts are shown in Table 17 at 60ºC.

Catalyst	S_{EtOH}^{TAEE}	S_{EtOH}^{ETBE}
A35 (E5)	0.130	0.870
CT275 (E9)	0.144	0.856

Table 17. Selectivity of ethanol for different catalysts.

Selectivity of ethanol to TAEE was slightly higher with CT275 than with A35 under the same operating conditions. CT275 presents higher average pore diameter than A35. This may explain that TAEE (bigger molecular size than ETBE) selectivity was enhanced using CT275.

The evolution of the selectivity in experimental run is represented in Figures 44 and 45, to observe if deactivation affects selectivity.

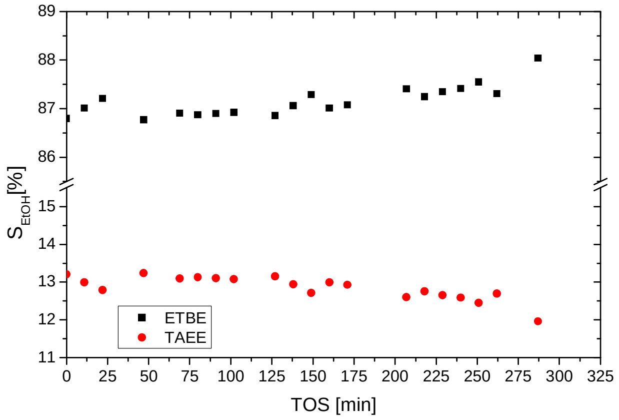

Figure 44. Ethanol selectivity evolution at T = 60ºC; [ACN] = 3100 ppm over A35.

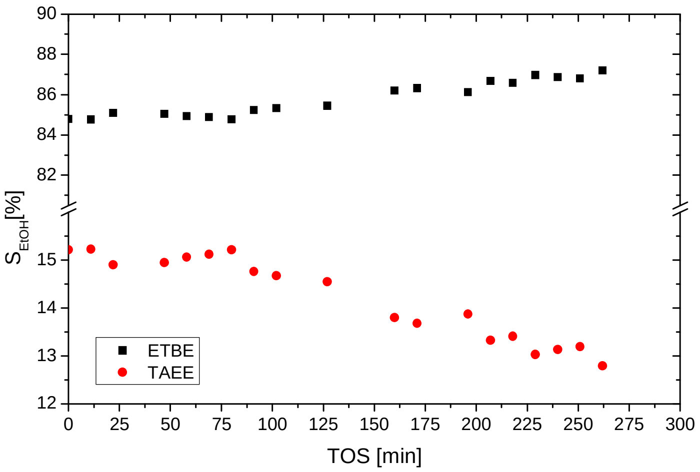

Figure 45. Ethanol selectivity evolution at T =80ºC; [ACN] =4000 ppm over A-35.

Figures 44 and 45 show an increase of selectivity of ethanol to ETBE in ACN presence. Then it is confirmed that ACN deactivation affects more TAEE production than ETBE production.

TBA was undetectable when ACN was present in the reaction system in all experiments without extra initial water. This is due to the reaction between ACN and water: water stops reacting with IB to react with ACN. Then, selectivity of IB only was studied at stationary state (before feeding ACN to the reactor). The effect of temperature, initial water content and type of catalysts was studied (fixed two parameters, the other was evaluated).

T [ºC]	S_{IB}^{TBA}
40	9.88 ± 0.21
60	8.33 ± 0.29
	8.63 ± 0.25
80	5.62 ± 0.14
	5.41 ± 0.13
	5.46 ± 0.11

Table 18. Effect of temperature on IB selectivity toward TBA without initial water addition on A35.

Temperature increase enhanced selectivity to ETBE. This means that ETBE reaction rate is more sensitive to temperature than TBA reaction rate (is more sensitive at temperature). Both reaction rates increased, but etherification of IB increased more than hydration of IB.

Initial water content [ppm]	$S_{IB \rightarrow TBA}$
0	8.63 ± 0.25
	8.33 ± 0.29
500	8.65 ± 0.14
2000	13.24 ± 0.61
4000	17.33 ± 0.15

Table 19. Effect of initial water content on selectivity at T=60ºC on A35.

Logically higher water content enhances the IB hydration to form TBA.

Catalyst	S_{IB}^{TBA}
A35	8.63 ± 0.25
CT275	5.67 ± 0.09

Table 20. Effect of catalyst on selectivity at T=60ºC without initial water addition.

4.9. Empirical Modelling of the Activity Decay

Reaction rate and activity decay curves are fitted by exponential equations. Exponential equation is shown in Equation 26 (where y-axis is activity or reaction rate and x-axis is time in minutes). Only the part with monotonically decrease of activity has been considered to be expressed as exponential-type equation, as follows:

$$y = a \exp(b \cdot x) \quad \text{Equation 26}$$

This type of equation corresponds to order 1 of deactivation. Annex 5 shows the fits for order 0 or lineal-type; order 1 or exponential-type and order 2 or hyperbolic-type [25]. The best was obtained for order 1.

In order to obtain the coefficients a and b, Eq.6 was fitted to experimental data. All obtained values are shown in Annex 6, for TAEE and ETBE respectively.

The values of coefficient b are almost equal for activity and for reaction rate. This fact is explained because the decreasing slope is the same. Coefficient a is the value of y-origin (when x=0, y=a) and it is different when fitting activity or reaction rate.

Figure 46 shows an example of the exponential fit realized with the software *CurveExpert 1.4*. Figure 47 show dependence among coefficient a and [ACN].

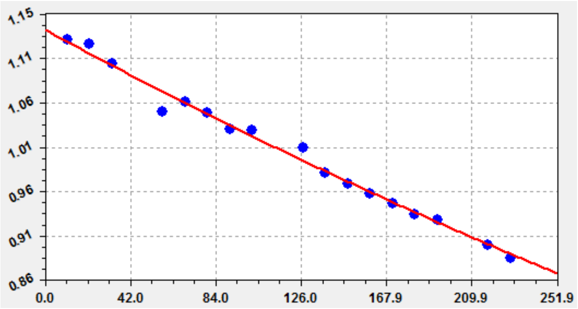

Figure 46. Example of the fitting of activity (y) versus time (x)

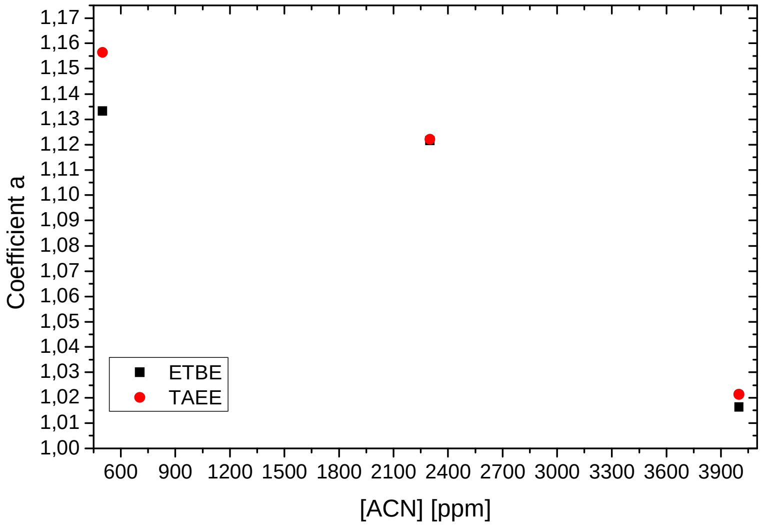

Figure 47. Coefficient *a* versus [ACN] for ETBE and TAEE at 80ºC.

The observed trend indicates that as [ACN] increases, the initial increase of activity (by water reaction) is lower as a consequence of higher deactivation rates.

Figure 48 shows the trend of coefficient b in front of [ACN].

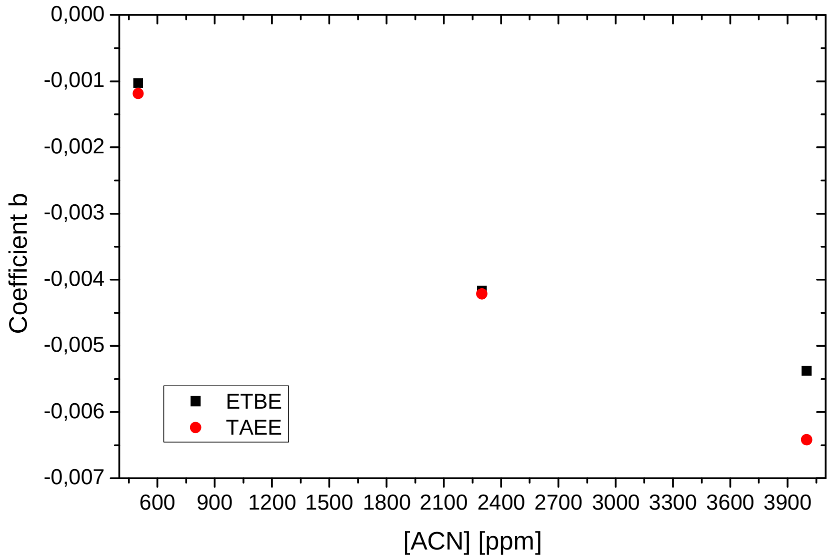

Figure 48. Coefficient *b* versus [ACN] for ETBE and TAEE at 80ºC

Coefficient *b* decreases (is more negative) on increasing [ACN]. Coefficient *b* more negative values means steeper decreasing slope: activity decreases faster at higher concentrations of ACN. This is due to the inhibitor effect of ACN.

Coefficients *a* and *b* changed also with temperature. Table 21 illustrates obtained values. Regression and standard error are shown in Annex 5.

Ether	Temperature [ºC]	Coefficient a	Coefficient b
TAEE	40	1.18	-0.0017
	80	1.02	-0.0064
ETBE	40	1.16	-0.0015
	80	1.02	-0.0054

Table 21. Coefficients for activity at different temperatures with same conditions (E4 and E6).

Coefficient *a* decreased when temperature increased. Activity increased more at first moment for low temperatures. This fact could be explained considering that high temperatures accelerated deactivation reactions.

Coefficient *b* decreased as temperature increased. In other words, activity decay was faster when higher was the temperature because high temperatures enhanced deactivation reactions. Both ethers presented similar values of coefficient *b*, but the trends indicated that ACN presence affected more TAEE than ETBE.

The effect of catalysts can be also observed comparing coefficients. Table 22 shows these data.

Products	Experiment	Coefficient a	Coefficient b
TAEE	E5 (A35)	1.235	-0.00242
	E9 (CT275)	1.148	-0.00240
ETBE	E5 (A35)	1.217	-0.00213
	E9 (CT275)	1.144	-0.00210

Table 22. Comparison of coefficients among A35 and CT275.

Coefficient *a* was higher for A35 than for CT275. The explanation may be due to the different average pore diameter of both catalysts: average pore diameter is higher for CT275 than for A35. Then, deactivation reactions started before in CT275 than in A35 because active sites were more accessible. Coefficient *b* was very similar for both catalysts. Values were somewhat lower for A35 than for CT275. Then it could be affirmed CT275 is more resistant to ACN deactivation than A35. The explanation may be due to the acid capacity. Acid capacity is higher for A35 than for CT275. Then, more acid catalyst is more sensitive to basic neutralization.

Figures 49 and 50 plot the trends of coefficients *a* and *b* respectively for different values of water concentration.

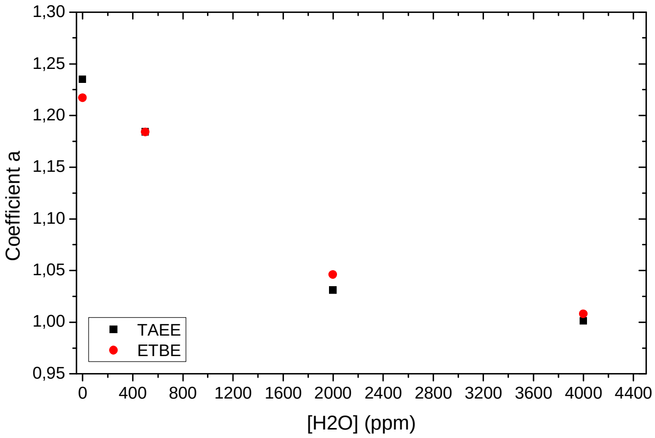

Figure 49. Coefficient *a* versus [H_2O] (3100 ppm ACN; 60ºC; A35).

Similar values of coefficient *a* were obtained for TAEE and ETBE. The presence of a higher amount of initial water seems to affect more to coefficient *a* for TAEE than that for ETBE case. TAEE has larger molecular size than ETBE.

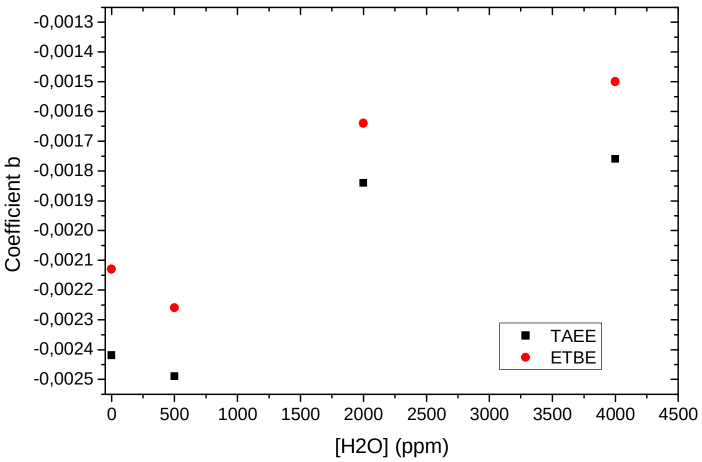

Figure 50. Coefficient b versus [H_2O] (3100 ppm; ACN; 60ºC; A35).

Coefficient b was smaller (more negative) for TAEE at any [H_2O] explored, including the case in with extra water was not added to the ethanol feed stream (first point). This means that TAEE is more sensitive at ACN presence, without dependence of water content in ethanol.

5. CONCLUSIONS

Deactivation of ion exchange resins in presence of acetonitrile

5 CONCLUSIONS

It has been confirmed the deactivation effect by ACN in IB and IA liquid-phase etherification with ethanol over ion exchange resins in a wide range of experimental conditions. Water inhibitory effect has been also observed in the present work.

Both etherifications are similarly affected by ACN presence, but TAEE production is slightly more affected than ETBE synthesis. Under the same experimental conditions, ETBE formation presents higher reaction rate than TAEE.

Both polymeric catalysts, Amberlyst^{TM} 35 WET (A35) and Purolite CT® 275 (CT-275), deactivate similarly in the presence of poison. Under the same experimental conditions, A35 presents higher catalytic activity than CT275.

The selectivity of ethanol to ETBE worsens when temperature increases.

Two different periods are observed in activity evolution when ACN enters inside the system: an initial period in which activity increase by water reaction with ACN, and a second period characterized by an exponential-type activity decrease. Deactivation in the second period is enhanced by temperature and deactivating agent concentration.

Finally, empirical model has been fitted to predict activity vas function of time in the exponential-type activity decay under the studied conditions.

Deactivation of ion exchange resins in presence of acetonitrile

6. REFERENCES AND NOTES

6 REFERENCES AND NOTES

1. Jordi Hug Badia i Córcoles, Carles Fité, Rafael González. Comportament de resines catalítiques en la síntesis d'ETBE davant de la presencia d'agents desactivadors, University of Barcelona (2010)
2. Timur Dogu, Dilek Varisli. Alcohols as Alternative to Petroleum for Environmentally Clean Fuels and Petrochemicals, Turk J Chem (2007).
3. http://en.wikipedia.org/wiki/OPEC
4. Meritxell Vila, Fidel Cunill, José Felipe Izquierdo, Javier Tejero, Montserrat Iborra. Equilibrium constants for Ethyl tert-Butyl Ether liquid-phase synthesis, Gordon and Breach Science Publishers S.A. (1993).
5. Rafael González Sánchez. Performance of Amberlyst^{TM} 35 in the synthesis of ETBE from ethanol and C_4 cuts. University of Barcelona. (2011).
6. José F. Izquierdo, Fidel Cunill, Meritxell Vila, Montserrat Iborra, Javier Tejero. Equilibrium Constants for Methyl tert-Butyl Ether and Ethyl tert-Butyl Ether Liquid-Phase Syntheses Using C_4 Olefinic Cut, Ind. Eng. Chem. Res. (1994).
7. Fidel Cunill, Meritxell Vila, José F. Izquiero, Montserrat Iborra, Javier Tejero. Effect of Water Presence on Methyl tert-Butyl Ether and Ethyl tert-Butyl Ether Liquid Phase Syntheses, Ind. Eng. Chem. Res. (1993).
8. http://www.quimicaorganica.net/sintesis-eteres-condensacion-alcoholes.html
9. R. Soto, C. Fité, E. Ramírez, R. Bringué, F. Cunill. Equilibrium of the simultaneous etherification of isobutene and isoamylenes with ethanol in liquid-phase, Elsevier (2014).
10. M. Umar, D. Patel, B. Saha. Kinetic studies of liquid-phase ethyl *tert*-butyl ether (ETBE) synthesis using macroporous and gelular ion exchange resin catalysts, Elsevier (2009).
11. http://www.efoa.eu/
12. R.Soto, C.Fité, E.Ramírez, J.Tejero, F.Cunill. Effect of water addition on the simultaneous liquid-phase etherification of isobutene and isoamylenes with ethanol over amberlyst^{TM} 35, Elsevier (2015).
13. J.H. Badia, C. Fité, R. Bringué, E. Ramírez, F. Cunill. Byproducts formation in the ethyl tert-butyl ether (ETBE) synthesis reaction on macroreticular acid ion-exchange resins, Elsevier (2013).
14. Carles Fité, Montserrat Iborra, Javier Tejero, José F. Izquierdo, Fidel Cunill. Kinetics of the Liquid-Phase Synthesis of Ethyl tert-Butyl Ether (ETBE), Ind. Eng. Chem. Res. (1994).
15. José Felipe Izquierdo, Fidel Cunill, Javier Tejero, Montserrat Iborra, Carles Fité. Cinética de las Reacciones Químicas. Edicions de la Universitat de Barcelona. Barcelona (2004).

16. Óscar Santín Pérez, Carles Fité Piquer, J.F. Izquierdo Torres. Estudio del control de las etapas físicas en las síntesis de MTBE y ETBE. University of Barcelona (2005).
17. Nezahat Boz, Timur Dogu, Kirali Murtezaoglu, Gulsen Dogu. Effect of hydrogen ion-exchange capacity on activity of resin catalyst in tert-amyl-ethyl-ether synthesis, Elsevier (2004).
18. http://encyclopedia2.thefreedictionary.com/Ion-Exchange+Resins
19. C. Fité, D.Parra, J.F. Izquierdo, F. Cunill, J. Tejero, M. Iborra, M. Vila. The effect of the reaction medium on the kinetics of the liquid-phase addition of methanol to isobutene. Elsevier (1998).
20. R. González, C. Fité, F. Cunill, K.D. Topp, R. Olsen. Deactivation of Ion Exchange Catalysts by Acetonitrile and Methylamine, Top Catal (2011).
21. Charles R. Marston. Improve Etherification Plant Efficiency and Safety. Identify Catalyst Deactivation Mechanism and Process Problems in MTBE/TAME/ETBE Production, The Dow Chemical Company (1994).
22. http://es.wikipedia.org/wiki/Polaridad_de_un_disolvente#Constante_diel.C3.A9ctrica_y_momento_dipolar.
23. R.Soto, C.Fité, E.Ramírez, J.H. Badia, R.Bringué, F.Cunill. Empirical kinetic model for the simultaneous liquid-phase etherification of isobutene and isoamylenes with ethanol over Amberlist 35^{TM}. Conference of ANQUE ICCE BIOTEC Madrid (2014).
24. Juha A. Linnekoski, Päivi Kiviranta-Pääkkönen, A.Outi Krause, Liisa K. Rihko-Struckmann. Simultaneous Isomerization and Etherification of Isoamylenes, Ind. Eng. Chem. Res. (1999).
25. Fogler, H.Scott. Elementos de ingeniería de las reacciones químicas. Pearson Educación, 3rd edition. México (2001).
26. Francesco Ancillotti, Marcello Massi Mauri, Ermanno Pescarollo, Luigi Romagnoni. Mechanisms in the reaction between olefins and alcohols catalyzed by ion exchange resins, Journal of Molecular Catalysis, Elsevier (1978).

7. ACRONYMS

7 ACRONYMS

1.	[ACN]	ACN concentration [ppm]
2.	[H_2O]	Water concentration [ppm]
3.	2M1B	2-Methyl-1-Butene
4.	2M2B	2-Methyl-2-Butene
5.	A	Pre-exponential factor
6.	A35	Macroporous ion exchange resin Amberlyst^{TM} 35 WET
7.	ACN	Acetonitrile
8.	B	Constant pre exponential
9.	BET	Brunauer-Emmet-Teller theory
10.	C_4	Olefin mixture composed mainly by compounds with 4 C atoms
11.	C_5	Olefin mixture composed mainly by compounds with 5 C atoms
12.	CAAA	Clean Air Act Amendments
13.	C_{AF}	Reactant concentration in fluid-phase [mol/L]
14.	C_{AS}	Reactant concentration at catalyst surface [mol/L]
15.	CO	Carbon monoxide
16.	CT275	Macroporous ion exchange resin Purolite CT275
17.	C_X	Concentration of X [mol/L]
18.	D	Internal diameter of reactor [mm]
19.	DEE	Diethyl ether
20.	DIB	Diisobutylene
21.	DIPE	Diisopropyl ether
22.	Dp	Diameter of particle [mm]
23.	DVB	Divinylbenzene
24.	E_{act}	Energy of activation [KJ/mol]
25.	EMT	External mass transfer
26.	Eq	Value at reaction equilibrium
27.	ETBE	Ethyl tert-butyl ether
28.	ETBE	Ethyl tert-butyl ether
29.	EtOH	Ethanol
30.	FCC	Fluid catalytic cracking
31.	FID	Flame ionization detector
32.	F_j	Molar flow of component j

33. GC	Gas chromatograph
34. GLC	Gas-Liquid Chromatograph
35. IA	Isoamylenes
36. IB	Isobutene
37. IMT	Internal mass transfer
38. IPTBE	Isopropyl tert-butyl ether
39. ISEC	Inverse Steric Exclusion Chromatography
40. k	Kinetic constant
41. K	Equilibrium constant
42. L	Bed length [mm]
43. LHSV	Liquid hourly space velocity [min^{-1}]
44. M_C	Catalyst mass [g]
45. MFC	Mass flow controller
46. M_{inert}	Inert mass [g]
47. MMA	Monomethylamine
48. MON	Motor Octane Number
49. MTBE	Methyl tert-butyl ether
50. NG	Natural gas
51. NO_X	Nitrogen oxides
52. P	Production annual (production of oil derivates)
53. PIC	Pressure indicator controller
54. PID	Proportional-integral-derivative controller
55. Q	Volumetric flow [mL/min]
56. R	Gas constant (8.314 [$J/(mol \cdot K)$])
57. r	Reaction rate [$mol/(kg_{cat} \cdot h)$]
58. R^2	Determination coefficient
59. $R_{j \to i}$	Molar ratio of compound j to compound i
60. RON	Research octane number
61. RR	Reserve of oil
62. Rvp	Raid vapour pressure [KPa or psi]
63. S	Standard Error
64. SC	Stream Cracking units
65. T	Temperature [K]

66. TAEE	tert-amyl ethyl ether
67. TAME	tert-amyl methyl ether
68. TCD	Thermo coupler detector
69. TIC	Temperature indicator controller
70. TMP-1	2,4,4-trimethyl 1-pentene
71. TMP-2	2,4,4-trimethyl 2-pentene
72. TOS	Time on stream [min]
73. V_B	Bed volume or reactor volume [mL]
74. VOC	Volatile organic compound
75. WHSV	Weight hourly space velocity [min^{-1}]
76. W_j	Mass flow of compound j [g/min]
77. X_j	Conversion of compound j
78. θ	Active site

8. ANNEXES

8. ANNEXES

8.1. ANNEX 1. EXPERIMENTAL CONDITIONS

Experiment	T [ºC]	[ACN] in ppm	[H2O] in ppm*	Catalyst
E1	80	2300	0	A35
E2	80	500	0	A35
E3	60	1100	0	A35
E4	80	4000	0	A35
E5	60	3100	0	A35
E6	40	4000	0	A35
E7	60	3100	4000	A35
E8	60	3100	2000	A35
E9	60	3100	0	CT275
E10	60	3100	500	A35

Table 23. Experimental Conditions

8.2. ANNEX 2. CHROMATOGRAPH CALIBRATION

8.2.1. Chromatograph Calibration Compositions

Compound	V1	V2	V3	V4	V5	V6	V7	V8	V9	V10
H2O	1.419	0.402	0.144	0.085	0.112	0.288	0	0.828	1.250	1.682
TAEE	6.630	4.365	2.165	3.346	1.062	0	7.955	10.41	13.98	5.166
TAA	1.155	1.297	0.505	0.441	0.210	0	0.324	0.691	0.201	2.422
TBA	2.273	1.567	0.543	0.619	0.594	0	0.734	1.258	0.460	2.243
ETBE	12.43	7.666	4.214	6.456	2.299	0	15.79	20.33	19.41	5.155
EtOH	32.30	46.69	34.06	31.21	38.07	44.41	36.58	47.53	16.30	23.77
ACN	0.185	0	1.111	0.342	0.640	0.148	0	0	0.107	0.076
2M1B	1.309	1.172	1.818	2.341	2.461	2.122	1.428	0.648	0.499	0.579
2M2B	19.79	17.72	27.48	35.40	37.20	32.08	21.59	9.804	7.544	8.751
IB	22.48	19.10	27.74	19.71	17.35	20.93	15.60	8.496	40.25	50.16

Table 24. Compositions (%m) calibrated with chromatograph.

8.2.2. Chromatograph Calibration Curves

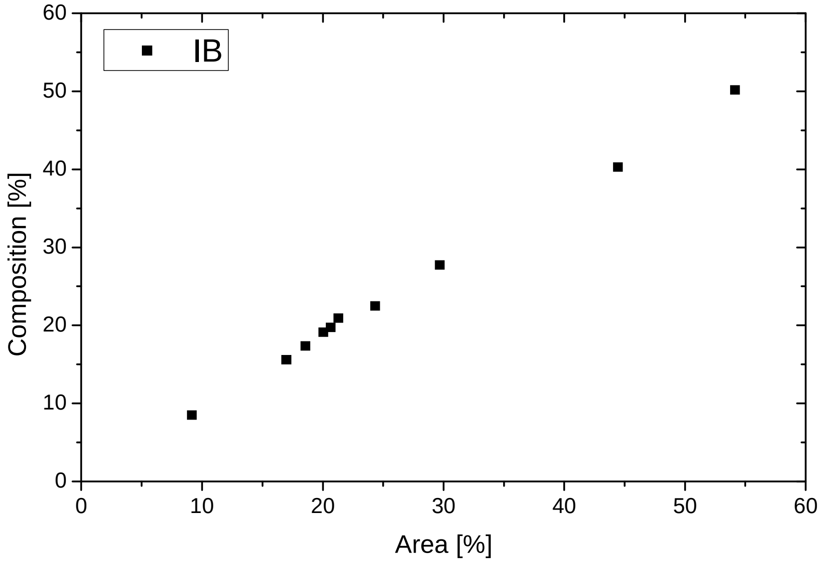

Figure 51. Isobutene curve

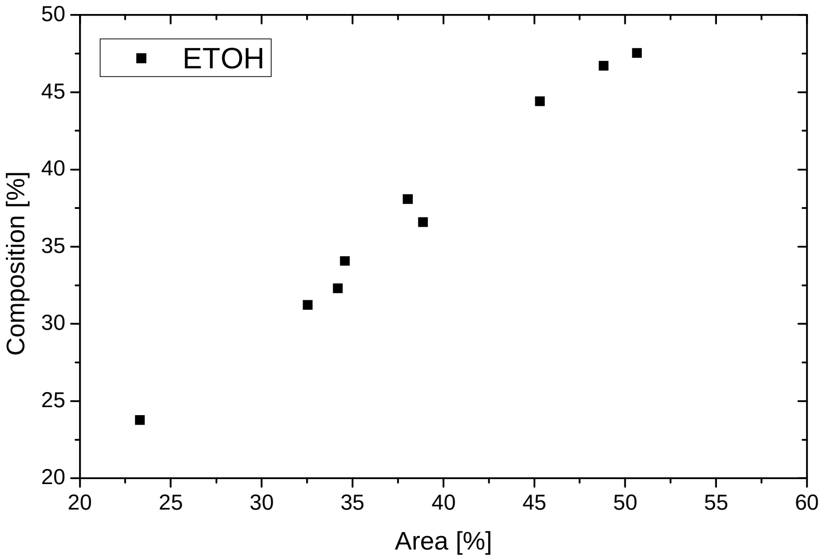

Figure 52. Ethanol curve

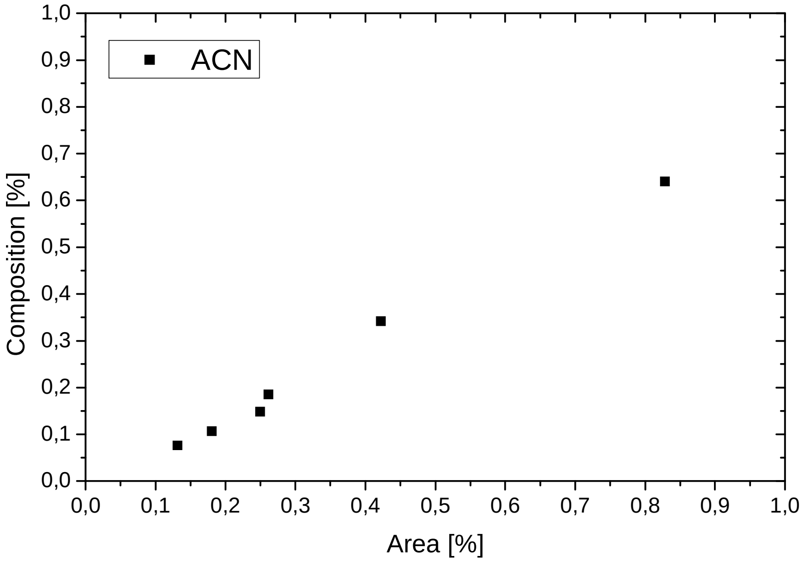

Figure 53. ACN curve

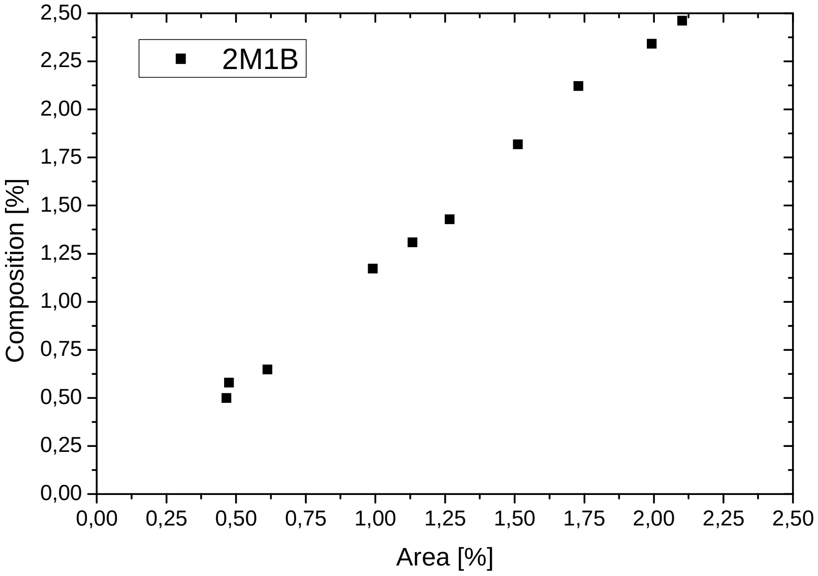

Figure 54. 2M1B curve

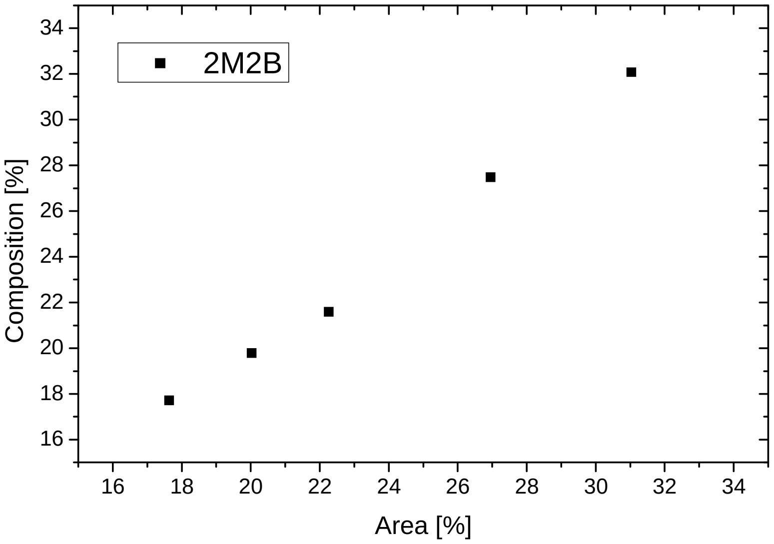

Figure 55. 2M2B curve

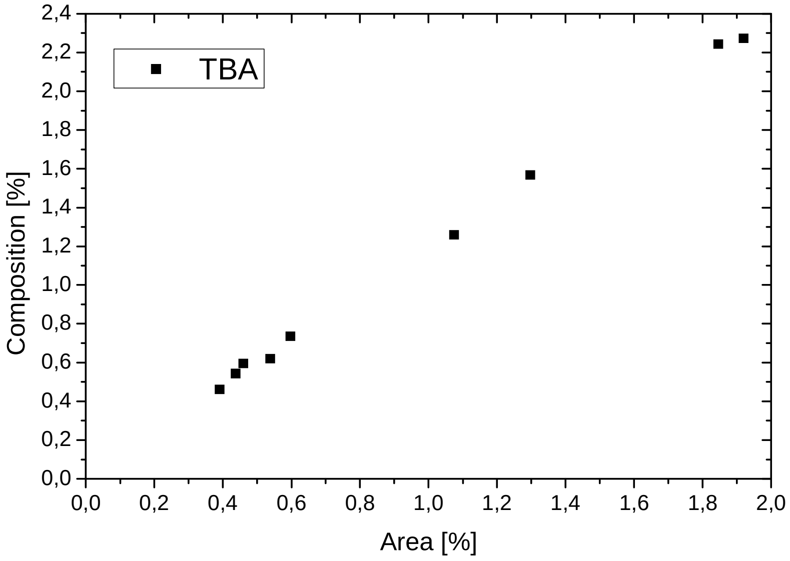

Figure 56. TBA curve

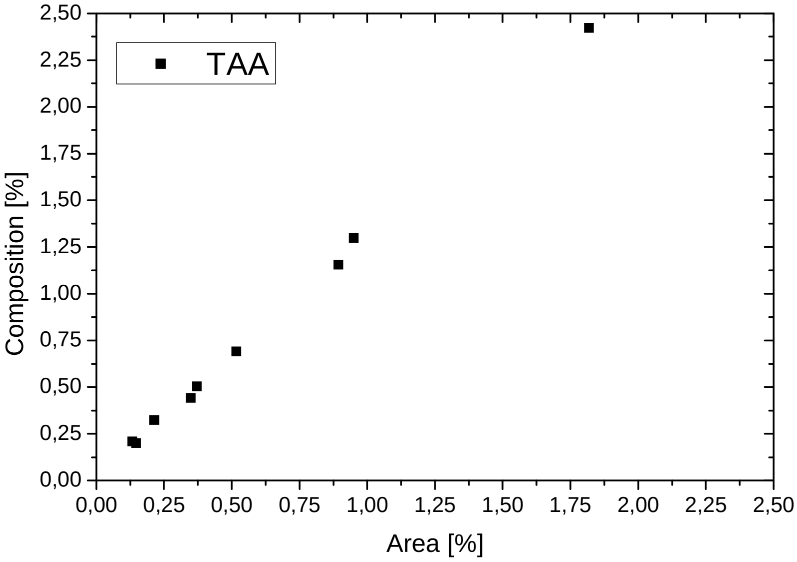

Figure 57. TAA curve

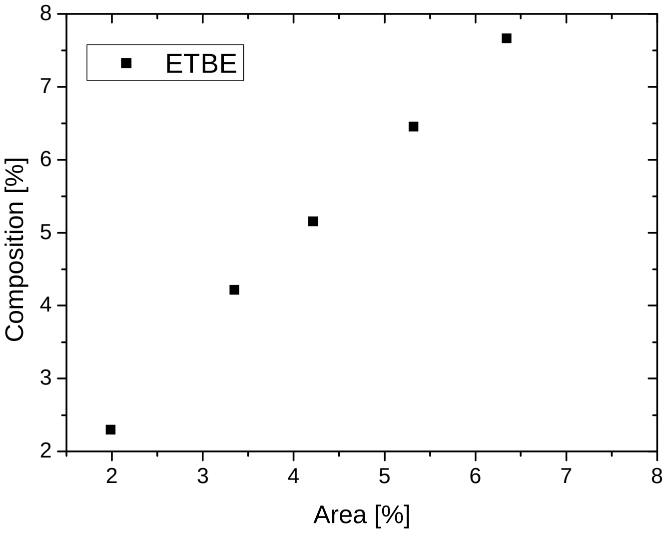

Figure 58. ETBE curve

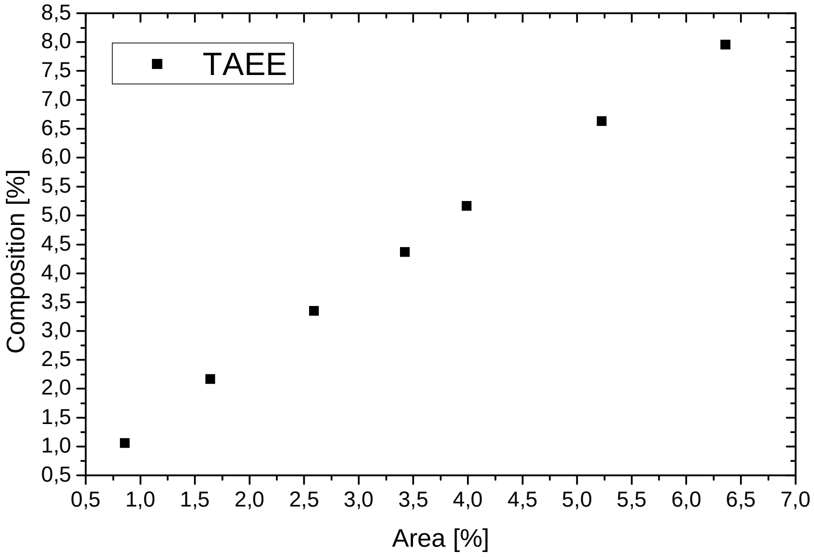

Figure 59. TAEE curve

8.3. ANNEX 3. PUMPS CALIBRATION

8.3.1. Pump 1 Calibration

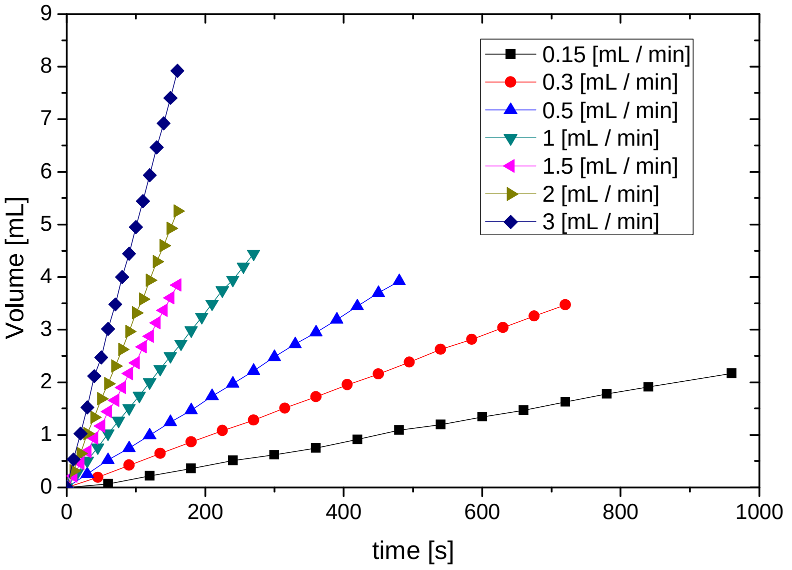

Figure 60. Obtaining of volumetric real flow pump 1.

PUMP	Q_{PUMP} [Ml/min]	Q_{REAL} [Ml/min]
PUMP 1	0.15	0.1392 ±0.000042
	0.3	0.2904 ±0.000022
	0.5	0.4902 ±0.000035
	1	0.9870 ±0.000080
	1.5	1.4532 ±0.00017
	2	1.9674 ±0.00021
	3	2.9514 ±0.00035

Table 25. Calibration of pump 1.

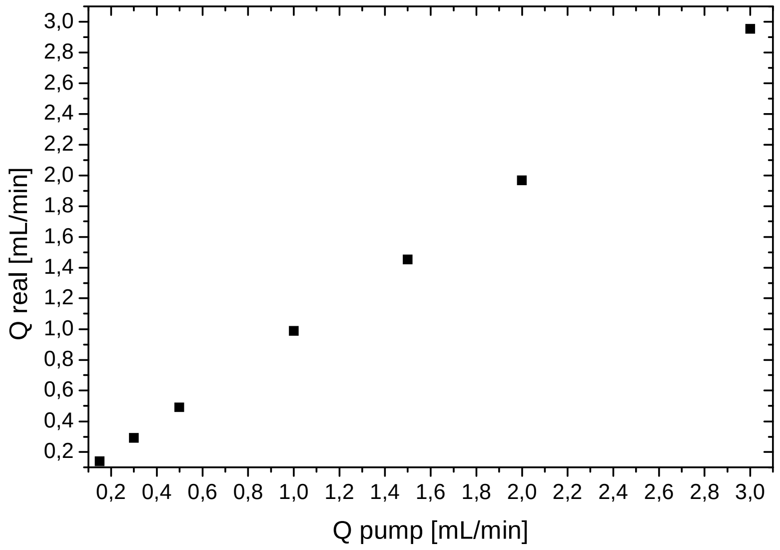

Figure 61. Pump 1 calibration curve.

8.3.2. Pump 2 Calibration

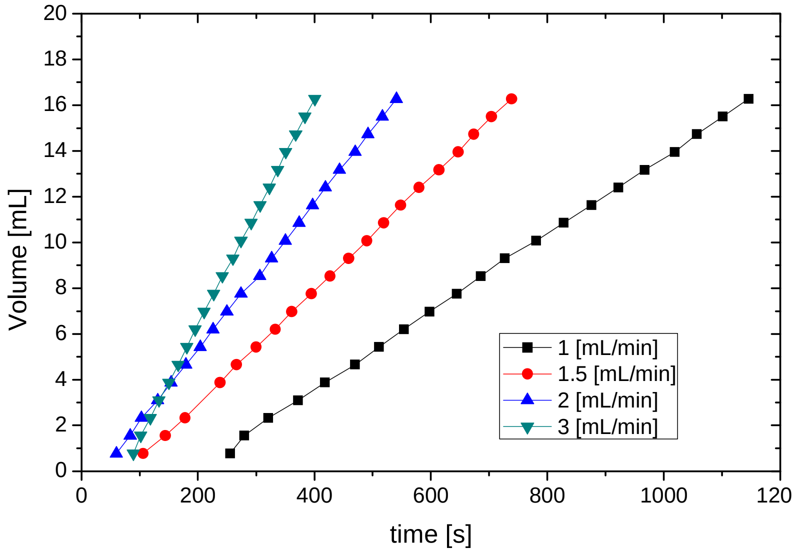

Figure 62. Obtaining of volumetric real flow pump 2.

PUMPS	Q_{PUMP} [Ml/min]	Q_{REAL} [Ml/min]
PUMP 2	1	1.023 ±0.000167
	1.5	1.484 ±0.00015
	2	1.925 ±0.000215
	3	2.973 ±0.000259

Table 26. Calibration of pump 2.

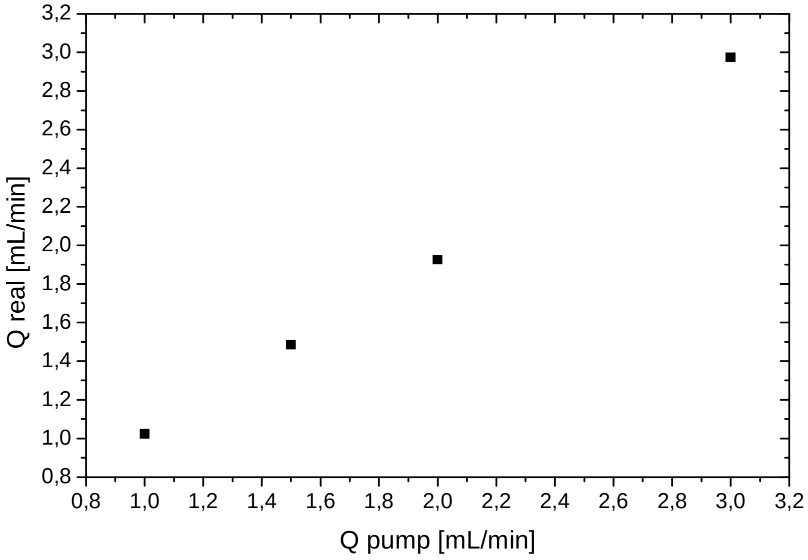

Figure 63. Pump 2 calibration curve.

8.4. ANNEX 4. KINETIC REACTION ORDER

The kinetic equations considered are shown in Equations 27 for ETBE formation and 28 for TAEE production.

$$r_{ETBE} = k\, C_{EtOH}^{X} C_{IB}^{Y} \quad \text{Equation 27}$$

$$r_{TAEE} = k\, C_{EtOH}^{X} C_{IA}^{Y} \quad \text{Equation 28}$$

Where kinetic constant is described by Equation 29 [25]

$$k = \exp(K_C + K_T(\frac{1}{T} - \frac{1}{\overline{T}}) \quad \text{Equation 29}$$

Where $\overline{T}$ is a medium value of temperature (60ºC or 333 K for the range of temperatures studied); exp (K_C) is the pre-exponential coefficient (named previously A) and K_T is ($-E_{act}/R$). Exponents X and Y, K_C and K_T were obtained by Solver, optimizing with experimental values of reaction rate by least squares regression.

Table 27 shows obtained activation energy by this method, comparing other values obtained from experimental reaction rates in this project and other values found in the literature.

Ether	E_{act} by Solver	E_{act} experimental	E_{act} literature
ETBE	75.2	73.0±3.0	77.5±11.0 [23]
TAEE	84.1	79.2±10.7	86.3±8.8 [23]

Table 27. E_{act} in units of [KJ/mol] fitted by Solver.

Table 28 shows obtained exponents X and Y and compare these values with literature.

Ether	Exponent	This project	Literature
ETBE	X	0.04	0 [26]
	Y	1.02	1 [26]
TAEE	X	0.04	0 [24]
	Y	0.88	1 [24]

Table 28. Exponents X and Y.

Table 29 shows calculated reaction rate and compare these values with experimental reaction rate.

Ether	T [ºC]	r_{exp}[mol/(kg$_{cat}$·h)]	r_{calc}[mol/(kg$_{cat}$·h)]
ETBE	40	31.35	27.02
	60	153.33	153.33
	80	714.61	714.61
TAEE	40	4.24	3.25
	60	22.64	22.64
	80	126.59	126.59

Table 29. Reaction rate calculated

8.5. ANNEX 5. DEACTIVATION ORDER

Order	Differential Equation	Integral Equation
0	$-\frac{da}{dt} = B_0$	$a=1-B_0 \cdot t$
1	$-\frac{da}{dt} = B_1 a$	$a=\exp(-B_1 \cdot t)$
2	$-\frac{da}{dt} = B_2 a^2$	$1/a=1+B_2 \cdot t$

Table 30. Deactivation order for activity (a) decay [25].

For order 0, activity (a) versus time is lineal-type. For order 1, ln(a) versus time is lineal-type. For order 2, (1/a) versus time is lineal-type. Figure 64 shows different fits for three orders.

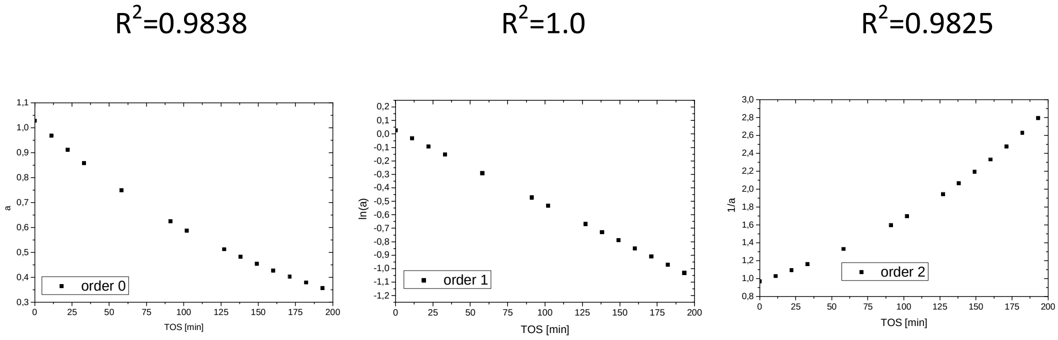

R^2=0.9838 R^2=1.0 R^2=0.9825

Figure 64. Deactivation orders.

As can be observed in Figure 64, order 1, where ln(a) is y-axis and TOS is x-axis, presents the best lineal trend. Then, ACN deactivation can be considered as order 1 deactivation.

Table 31 shows the values of B_0, B_1 and B_2 obtained by Solver fit.

B	Values
B_0	0.00385
B_1	0.00548
B_2	0.00785

Table 31. Values of constants at different deactivation orders.

8.6. ANNEX 6. FIT COEFFICIENTS

Experiments	A	b	R^2	S
E1	1.122	-0.00422	0.998	0.0135
E2	1.157	-0.00119	0.986	0.0159
E3	1.330	-0.00098	0.983	0.0141
E4	1.021	-0.00642	0.998	0.0180
E5	1.235	-0.00242	0.997	0.0133
E6	1.184	-0.00170	0.992	0.0165
E7	1.001	-0.00176	0.985	0.0228
E8	1.031	-0.00184	0.954	0.0403
E9	1.148	-0.00240	0.991	0.0217
E10	1.184	-0.00249	0.994	0.0195

Table 32. Coefficients *a* and *b* for TAEE's activity.

Experiments	a [mol/(h·kg_{cat})]	b	R^2	S
E1	125.4	-0.00417	0.997	1.899
E2	163.1	-0.00124	0.991	1.725
E3	29.1	-0.00098	0.983	0.309
E4	130.1	-0.00641	0.998	2.277
E5	28.9	-0.00242	0.997	0.312
E6	5.0	-0.00170	0.992	0.070
E7	17.7	-0.00172	0.993	0.280
E8	23.3	-0.00194	0.981	0.632
E9	24.2	-0.00239	0.991	0.471
E10	28.6	-0.00247	0.991	0.587

Table 33. Coefficients *a* and *b* for TAEE's reaction rate.

Experiments	A	b	R^2	S
E1	1.122	-0.00417	0.998	0.0135
E2	1.133	-0.00103	0.990	0.0116
E3	1.288	-0.00082	0.984	0.0113
E4	1.016	-0.00538	0.998	0.0138
E5	1.217	-0.00213	0.998	0.0089
E6	1.157	-0.00146	0.995	0.0106
E7	1.008	-0.00150	0.998	0.0066
E8	1.046	-0.00164	0.988	0.0195
E9	1.144	-0.00210	0.998	0.0086
E10	1.184	-0.00226	0.997	0.0123

Table 34. Coefficients *a* and *b* for ETBE's activity.

Experiments	a [mol/(h·kg$_{cat}$)]	B	R^2	S
E1	709.7	-0.00349	0.998	7.070
E2	899.8	-0.00103	0.990	9.215
E3	193.3	-0.00082	0.984	0.984
E4	726.9	-0.00538	0.998	9.933
E5	190.5	-0.00213	0.998	1.392
E6	36.3	-0.00146	0.995	0.334
E7	119.4	-0.00150	0.998	0.788
E8	150.7	-0.00152	0.972	4.226
E9	143.4	-0.00209	0.997	1.331
E10	188.0	-0.00223	0.995	2.493

Table 35. Coefficients *a* and *b* for ETBE's reaction rate.

As it can be observed, experimental data fit to the proposed equations in a remarkable good fashion with low values of standard error.